Triassic–Paleogene paleogeography of the Arctic: Implications for sediment routing and basin fill

Article *in* AAPG Bulletin · November 2018

DOI: 10.1306/05111817254

1 author:

Tor O Somme
Equinor ASA

Triassic–Paleogene paleogeography of the Arctic: Implications for sediment routing and basin fill

T. O. Sømme, A. G. Doré, E. R. Lundin, and B. O. Tørudbakken

ABSTRACT

Predicting the lateral distribution of petroleum play elements (reservoirs, source rocks, and seals) requires basic understanding of regional basin evolution and depositional history. In remote areas where little data are available or where the basins have undergone episodes of tectonic deformation, this understanding relies on integrated analysis of the plate tectonic framework and the resulting paleogeography. The Arctic has experienced several episodes of tectonic deformation, which fundamentally changed the basin configuration and patterns of sediment routing. Here, we present a set of paleogeographic maps highlighting these changes during the Triassic–Paleogene. In the Triassic, the Arctic was characterized by a central restricted basin, which predominantly received clastic input from the Polar Urals and Arctic Canada. The Alaskan and Siberian passive margins received clastics from continent-scale drainage systems extending into the North American craton and the central Asian fold belt, respectively. In the Jurassic, the region was dominated by rifting as the central Arctic landmass rifted away from Laurentia. In the Early Cretaceous, the northern margin of the Barents Sea underwent regional uplift resulting in new provenance areas shedding sediments southward. Compression along the Pacific margin formed continuous topography and high sediment input to the Canada Basin during the Late Cretaceous. Regression in the Canada Basin continued in the Paleogene when major rift–tip deltas formed. This overview of Arctic paleogeography demonstrates the complexity of this overall data-poor area and shows the need for integrated, regional models to understand sediment routing and stratigraphic development in such areas.

Manuscript received June 13, 2017; provisional acceptance August 17, 2017; revised manuscript received September 12, 2017; revised manuscript provisional acceptance January 11, 2018; final acceptance May 11, 2018.
DOI:10.1306/05111817254

AUTHORS

T. O. Sømme ~ *Equinor ASA, Martin Linges vei 33, 1364 Fornebu, Norway; tooso@equinor.com*

T. O. Sømme received his M.Sc. in 2005 and his Ph.D. in 2009 from the University of Bergen. He has worked at Statoil (now Equinor) as an exploration geologist since 2012. His main interest is stratigraphic analysis of sedimentary basins and the link to onshore sediment-routing systems.

A. G. Doré ~ *Equinor UK Limited, One Kingdom Street, London W2 6BD, United Kingdom; agdo@equinor.com*

A. G. Doré received his B.Sc. and his Ph.D. from University College London, and has held several technical and leadership positions in the oil industry. He currently advises Equinor's exploration management, with a global remit. He has worked extensively in northwest Europe, the Atlantic, and the Arctic, and his current interests include uplifted petroleum systems, passive margin structure, and cratonic basins.

E. R. Lundin ~ *Equinor ASA, Arkitekt Ebbells veg 10, 7053 Trondheim, Norway; erlun@equinor.com*

E. R. Lundin is an exploration geologist at Equinor. He received his B.S. (1984) from Fort Lewis College, his M.S. (1987) from the University of Arizona, and his Dr.Philos. (2008) from the University of Oslo. His main interests are structural geology, regional geology, and tectonics. He has worked extensively in the Atlantic and the Arctic.

B. O. Tørudbakken ~ *Equinor ASA, Martin Linges vei 33, 1364 Fornebu, Norway; boto@equinor.com*

B. O. Tørudbakken received his Cand.real. from the University of Oslo in 1982. After 4 years in academia, he started in the oil industry in 1986. He is presently working with international exploration at Equinor. His main interests are regional geology and exploration concepts.

ACKNOWLEDGMENTS

The ideas discussed in this paper are based on knowledge and contribution from many colleagues, and we acknowledge

Ana D. Gibbons, Gillian D. Dale, Elisabeth Bjerkebæk, Bart Hendriks, Antonina Stupakova, Erik P. Johannessen, Jonas Wilson, Torbjørn Dahlgren, Jakob Skogseid, Anna-Jayne Zachariah, Ian Lunt, Helge K. Gjelberg, Sverre Henriksen, and Alf E. Ryseth. We thank ION Geophysical Corporation, the Norwegian Petroleum Directorate, and WesternGeco for permission to publish seismic data. Owen Anfinson, Edward J. Fleming, Bernard Coakley, and AAPG Editor Barry J. Katz provided valuable comments that improved the clarity of the manuscript.

INTRODUCTION

The Arctic holds some of the most prolific petroleum basins in the world, with proven resource estimates amounting to approximately 10% of the world's total and with an additional 90 billion bbl of oil and 1669 trillion ft^3 of natural gas yet to be found (Bird et al., 2008). These proven resources are largely concentrated in areas such as the West Siberia Basin in Russia, the North Slope of Alaska, and the Norwegian Barents Sea (Figure 1). The remaining parts of the Arctic are largely underexplored, located far away from settlements and infrastructure in some of the harshest climate conditions on the planet. Prospectivity assessment in these remote areas of the Arctic is challenging because of the lack of dense seismic and well data, so that prediction of petroleum play elements such as reservoirs, source rocks, and seals largely relies on conceptual subsurface models.

Paleogeographic models aim to describe the distribution of topography, bathymetry, and overall depositional environments in ancient landscapes and seascapes. The temporal and spatial variability in sediment flux, subsidence rates, and along-strike distribution of sediment entry points controls stratal geometries and the distribution of potential reservoir bodies, source rocks, and seals in the subsurface. More specifically, siliciclastic reservoir quality is linked to the mineralogy and textural maturity of the sediment prior to burial, reflecting the lithology of the provenance area, climate conditions at the time of deposition, and transport distance from the hinterland to the site of deposition (Johnsson, 1993). The volume of sediment that is being produced in the hinterland is primarily controlled by the size of river catchments, the relief, climate, and basement lithology (e.g., Syvitski and Milliman, 2007; Portenga and Bierman, 2011). In the distal end of the system, width and along-strike distribution of facies belts and the run-out distance of basin-floor fan systems scale to the morphometrics of the onshore part of the routing system (Sømme et al., 2009). An integrated understanding of the paleogeography of ancient landscapes and seascapes is therefore critical for predicting basin stratigraphy through time.

The Pangean Arctic landmass was a result of late Paleozoic assemblage of several different tectonic blocks and terranes (e.g., Torsvik and Cocks, 2004; Lawver et al., 2011). During the pre-Mesozoic time, the Arctic was dominated by carbonate deposition (e.g., Golonka et al., 2003; Golonka, 2011). A major change occurred at the Paleozoic–Mesozoic transition when the Pangean topography was denuded and large volumes of clastics were transported to the surrounding basins (Figure 2). Subsequent fragmentation of the Arctic Pangea was a consequence of subduction, slab rollback, and back-arc extension along the paleo-Pacific margin (Nokleberg et al., 2001; Hamilton, 2007; Kuzmichev, 2009).

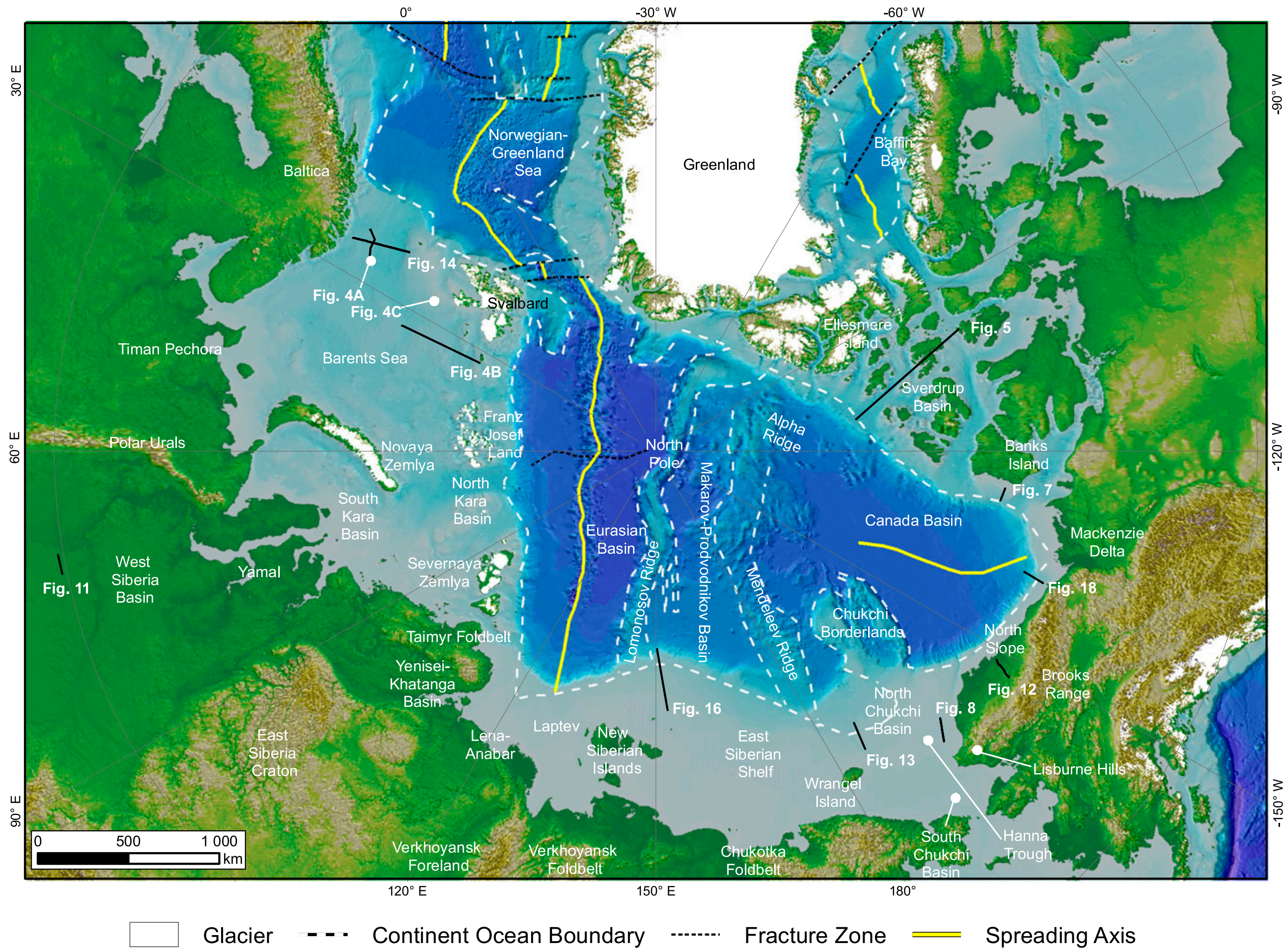

Figure 1. Present-day topographic and bathymetric map of the Arctic highlighting key structural features and geographic regions mentioned in the text.

The combination of a complex plate tectonic setting and the scarcity of data in and around the Canadian and the Eurasian Basins have resulted in the proposal of several distinct models of the post-Pangean breakup of the Arctic (e.g., Herron et al., 1974; Grantz et al., 1979; Dutro, 1981; Miller et al., 2006; Kuzmichev, 2009). Application of any of these models has direct consequences for prospectivity assessment in these Arctic regions by controlling the timing and distribution of onshore topography as well as tectonic deformation and subsidence patterns in the offshore basins.

Here, we present a set of new paleogeographic maps covering the breakup of the Arctic Pangea from the Triassic to the Paleogene during the time the Arctic was dominated by siliciclastic deposition. This work is part of a larger study that was conducted internally by Statoil (now Equinor), which aimed to produce a coherent view of the plate-tectonic and paleogeographic evolution of the Arctic. The maps presented here are based on the plate-tectonic framework presented in Doré et al. (2015). This framework uses a three-stage opening model for the Arctic, which includes opening of the Canada Basin (e.g., Grantz et al., 1979), followed by successive opening of the Makarov–Podvodnikov and Eurasia Basins (e.g., Alvey et al., 2008). This model has been refined with respect to plate boundaries, structural elements, and timing of plate movements based on interpretation of gravity and magnetic data, stratigraphic information, and available magmatic ages (see Doré et al., 2015 for more details). Because some of the tectonic plates crossed the North Pole and changed their relative orientation during the opening of the Canada and Eurasia Basins, all geographical references cited in the text refers to paleolatitudes at the time of deposition.

Superimposed on this plate-tectonic framework, paleogeographic environments are based on

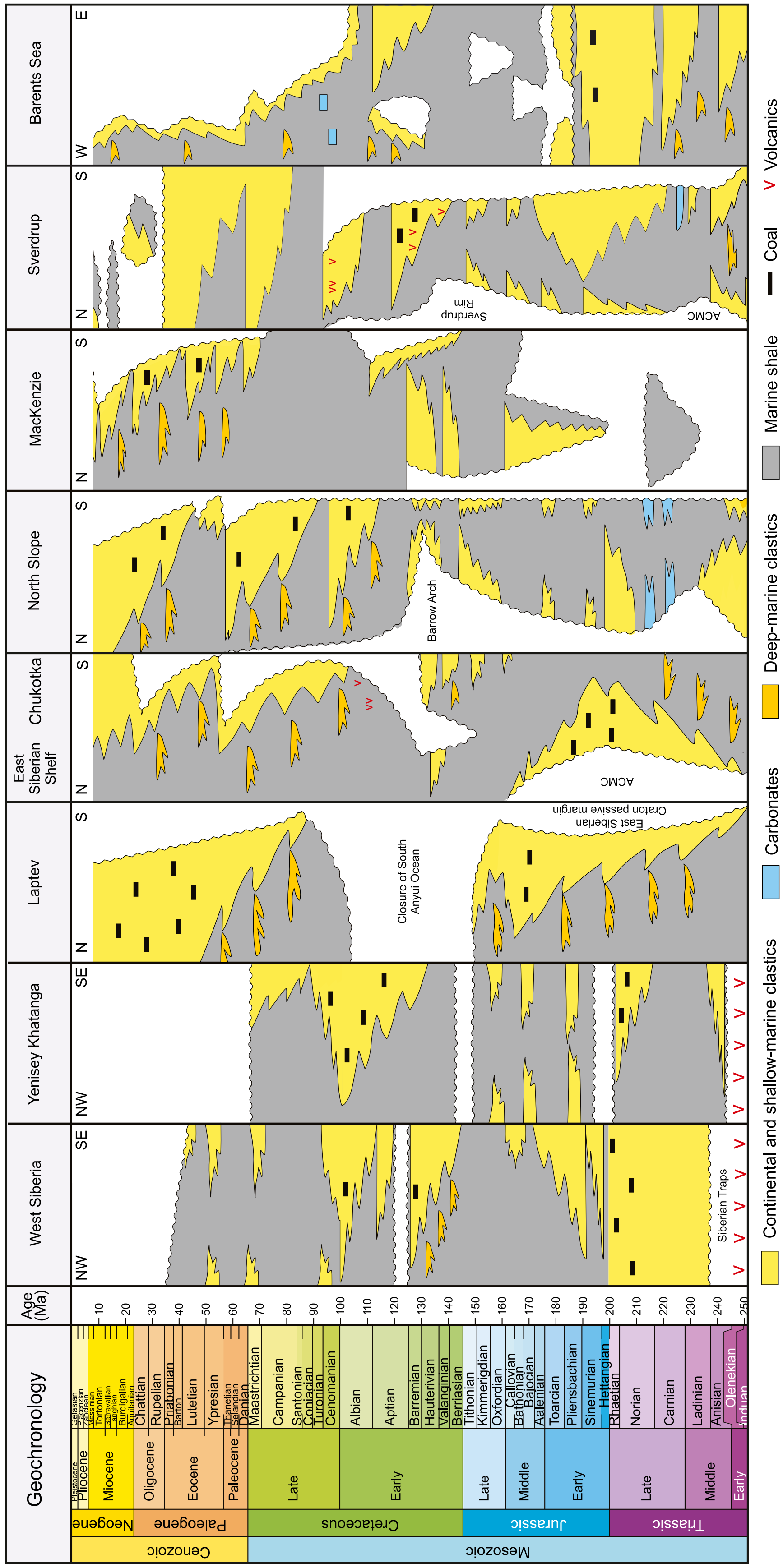

Figure 2. Simplified chronostratigraphy for key regions discussed in the text. The diagram illustrates the main transgressive and regressive events and changes in sediment source area for different basins. Note that the geographical orientations refer to present-day coordinates, whereas paleocoordinates are used in the text. Modified from Dixon (1996), Egorov and Mørk (2000), Sekretov, (2001), Vyssotski et al. (2006), Dewing and Embry (2007), Miller and Verzhbitsky (2009), Drachev (2011), Houseknecht and Bird (2011), Kontorovich et al. (2013, 2014). ACMC = Alaska–Chukotka microcontinent.

interpretation of seismic reflection and well data, supplemented by published seismic, well, and outcrop information. Constraints on timing of tectonic uplift and deformation of sediment source areas are based on structural information and published fission track thermochronology data. A review of published detrital zircon provenance data is used to help delineate main sediment-routing systems through time. The maps were constructed by rotating time-specific data points (e.g., from wells, seismic or outcrop) to their paleoposition using the plate model described earlier in the section. To maintain consistency between data-rich and data-poor regions, we describe a limited number of paleoenvironments that are associated with specific facies association types. Where the transition between paleoenvironments cannot be determined from seismic reflection or well data, global-scaling relationships (sensu Sømme et al., 2009) have been used to determine the extent of paleoenvironments based on tectonic setting and type of sediment-routing system.

"Constructive topography" refers to areas that are undergoing tectonic deformation and where the relative topography is increasing, whereas "destructive topography" refers to areas where deformation has ceased and where the topography is decreasing by denudation. "Alluvial plain" describes continental deposition and "lakes" refer to large onshore water bodies detached from the sea. "Marginal marine" describes near-coastal environments that experience rapid shifts in facies belts during high-frequency relative sea-level fluctuations, and the "shelf" is the area that is repeatedly emerged and submerged during sea-level changes. In pre-Cenozoic greenhouse times, the water depth on the shelf was probably around or less than 50 m (164 ft). The "slope" marks the transition between the "shelf" and the "basin floor." The basin floor is dominated by fine-grained hemipelagics and coarser gravity flow deposits fed from nearby fluvial systems. The water depth in the basin floor environment probably ranged between a few hundred meters to several kilometers depending on basin setting (intracratonic, extensional rift, passive margin, or arc-related).

TRIASSIC

The transition from the Paleozoic to the Mesozoic marked a major change in tectonic style and depositional conditions in the Arctic (Golonka, 2011). The Triassic was characterized by regression in many areas (Figures 2, 3). The Uralian orogeny was in its final phase and the Taimyr area also experienced late stage compression, which continued into the Triassic (Inger et al., 1999; Torsvik and Andersen, 2002; Puchkov, 2013; Toro et al., 2016). At the Permian–Triassic boundary, Siberian Traps flood basalts (Figure 2) covered the area between the East Siberian craton, the Polar Urals and the Lena–Anabar region, extending as far north as the northern part of the South Kara Basin (Buslov et al., 2010). Late Paleozoic uplift probably caused the southeastern part of the West Siberia Basin to be subaerially exposed, forming a network of erosional valleys that supplied sediment to the South Kara and Yenisei–Khatanga Basins. Outcrops on Novaya Zemlya document marginal-marine and continental deposition during the Early Triassic (e.g., Gramberg, 1988), and it is inferred that the region may have bypassed clastic material to the eastern Barents Sea and North Kara Basin prior to uplift of Novaya Zemlya in the Late Triassic–Early Jurassic (long-hatched routing system in Figure 3) (Stoupakova et al., 2011; Toro et al., 2016).

Subsidence in the West Siberia Basin, Yamal and South Kara Basin regions probably started in the Middle Triassic when the basin was transgressed through the Yenisei–Khatanga Basin. These basins were dominated by continental, shallow lacustrine and shallow-marine environments, surrounded by near-coastal and fluvial systems prone to coal deposition (Vyssotski et al., 2006). The basins probably captured fluvial systems from a broad area, beginning with local highs in the Polar Urals, Taimyr, and the North Kara Basin areas (Daragan-Sushchova et al., 2014), and eventually expanding to the tectonically active Novaya Zemlya area toward the end of the Triassic. On the southern margin of the Yenisei–Khatanga Basin, the Lower and Middle Triassic succession is dominated by shallow-marine and nearshore deposits (Egorov and Mørk, 2000). In contrast to other Arctic basins, which experienced Triassic regression (e.g., the Barents Sea and Sverdrup Basins), the sediment flux to the Yenisey–Khatanga Basin appears to have been relatively low and the area was dominated by overall transgression during the Early and Middle Triassic (Figure 2) (Egorov and Mørk, 2000). Despite relatively low sediment input, detrital zircon data from the Triassic deposits in

Figure 3. The Triassic was dominated by overall regression. The paleo-Pacific was characterized by deep-water, passive margin conditions receiving sediments from large Laurentian and Siberian rivers. The relatively shallow, intracratonic central Arctic basin was mainly supplied not only from the Polar Urals, but also from other local sediment source areas. The Alaska-Chukotka microcontinent was a relatively small source area feeding sediment into the Sverdrup Basin, the Hanna trough area and the South Anyui ocean. The long-dashed routing system illustrates possible sediment transport from the West Siberia Basin to the North Kara Basin and eastern Barents Sea prior to Late Triassic–Early Jurassic uplift of Novaya Zemlya. The short-dashed routing system illustrates the trans-Arctic routing system as suggested by, for example, Miller et al. (2013) and Anfinson et al. (2016). F.J.L. = Franz Josef Land; NSI = New Siberian Islands; WI = Wrangel Island.

Yenisey–Khatanga indicate that Taimyr was the main sediment source area (Zhang et al., 2016).

Sandy shallow and marginal-marine clastics also dominated the Lena–Anabar area to the east (Egorov and Mørk, 2000), marking the transition from the confined Yenisei–Khatanga Basin, to a wide, deep-water South Anyui ocean (Figure 3) (Oxman, 2003; Khudoley and Prokopiev, 2007). The presence of what appear to be Late Jurassic ophiolites on the New Siberian Islands (Kuzmichev, 2009) suggests that the South Anyui ocean was at least partly floored by oceanic crust and was an embayment of the proto-Pacific at the time. This is also documented by outcropping Permian to Jurassic rocks in the Verkhoyansk fold belt at the flank of the East Siberian craton, where the Permian–Triassic succession is dominated by several kilometers of shallow and deep-water clastics deposited in a passive margin setting (Figure 2) (Khudoley and Guriev, 1994; Egorov and Mørk, 2000; Konstantinovsky and Lipchanskaya, 2011; Ershova et al., 2016). Detrital zircon data derived from the same Triassic deep-water sandstones show that this margin was supplied by extensive river systems sourced from the central Asian fold belt (Figure 3) (Prokopiev et al., 2008).

Late Triassic to Early Jurassic compression and deformation in the Polar Urals, Novaya Zemlya, and Taimyr areas (Figure 3) (Toro et al., 2016) created high topography and sediment production along the mountain belt. Initial subsidence in the West Siberia Basin led to onlap and backfilling of the late Paleozoic and Early Triassic erosional landscape, resulting in decreasing sediment input from the southeast. On the southwestern flank of Novaya Zemlya, well and seismic reflection data show that the Barents Sea was characterized by prolonged and regional regression (Figure 2), where the rate of sediment delivery outpaced the rate of subsidence and accommodation generation (Figure 4A, B).

In the western Barents Sea, mapping of discrete shelf-break positions demonstrates approximately 700 km (~430 mi) of Triassic regression from the Induan to the Carnian (Henriksen et al., 2011; Lundschien et al., 2014). Seismic data also suggest that the Triassic depositional system probably did not prograde beyond Svalbard (Høy and Lundschien, 2011), before the basin transgressed in the Norian (Figure 4A). Outcropping Upper Triassic (Carnian and Norian) strata on Svalbard and the surrounding islands document mainly shelfal and minor shallow-marine and continental deposits (Figure 4C) (Riis et al., 2008; Klausen and Mørk, 2014; Lundschien et al., 2014; Vigran et al., 2014). A narrow marine to continental Triassic basin also extended southward between Greenland and Baltica (Müller et al., 2005).

The Triassic was also dominated by major regression further east in the Barents Sea and similar to Svalbard, the Late Triassic (Norian) succession on Franz Josef Land documents shelfal and marginal-marine deposits (Dypvik et al., 1998). But in contrast to the outcrops on Svalbard, it has been suggested that these deposits were sourced from the Taimyr area to the north based on facies relationships and detrital zircon data (Dibner, 1998; Soloviev et al., 2015). Triassic regression is also well documented in the easternmost part of the Barents Sea and in the Timan–Pechora area, where Middle to Upper Triassic rocks comprise stacked continental and nearshore, fine-grained sandstones and shales (Tugarova et al., 2008; Kaminsky et al., 2011). Regional regression in this area may have started already in the late Permian and well and seismic data suggest the development of an early clastic dispersal system. Together these observations indicate that an open ocean basin existed between the terminal regressive system in the Barents Sea and the Sverdrup Basin, but that a land area existed farther north in the Triassic (Figure 3) (Anfinson et al., 2016). Preservation of a central Arctic intracratonic sea in the latest Triassic is also suggested from paleontological data (Zakharov et al., 2002) and by outcrops on the New Siberian Islands, where thick units of marine shales suggest depositional conditions distal from major sediment sources (Kos'ko and Korago, 2009). Egorov and Mørk (2000) also highlighted a remarkable similarity of the Triassic successions in the Barents Sea, Sverdrup and Yenisei–Khatanga Basins, pointing toward a common first-order control on deposition in these areas.

Seismic mapping of progradational shelf–slope wedges (e.g., Glørstad-Clark et al., 2010; Eide et al., 2018) and an increasing volume of provenance data from the Triassic succession in the Barents Sea, Svalbard, and Franz Josef Land show that the primary sediment source area for the regional Triassic regression was the Polar Urals, with additional contribution from Novaya Zemlya and Baltica (Figure 3) (Bue and Andresen, 2014; Soloviev et al., 2015; Fleming et al., 2016; Klausen et al., 2017). Work by

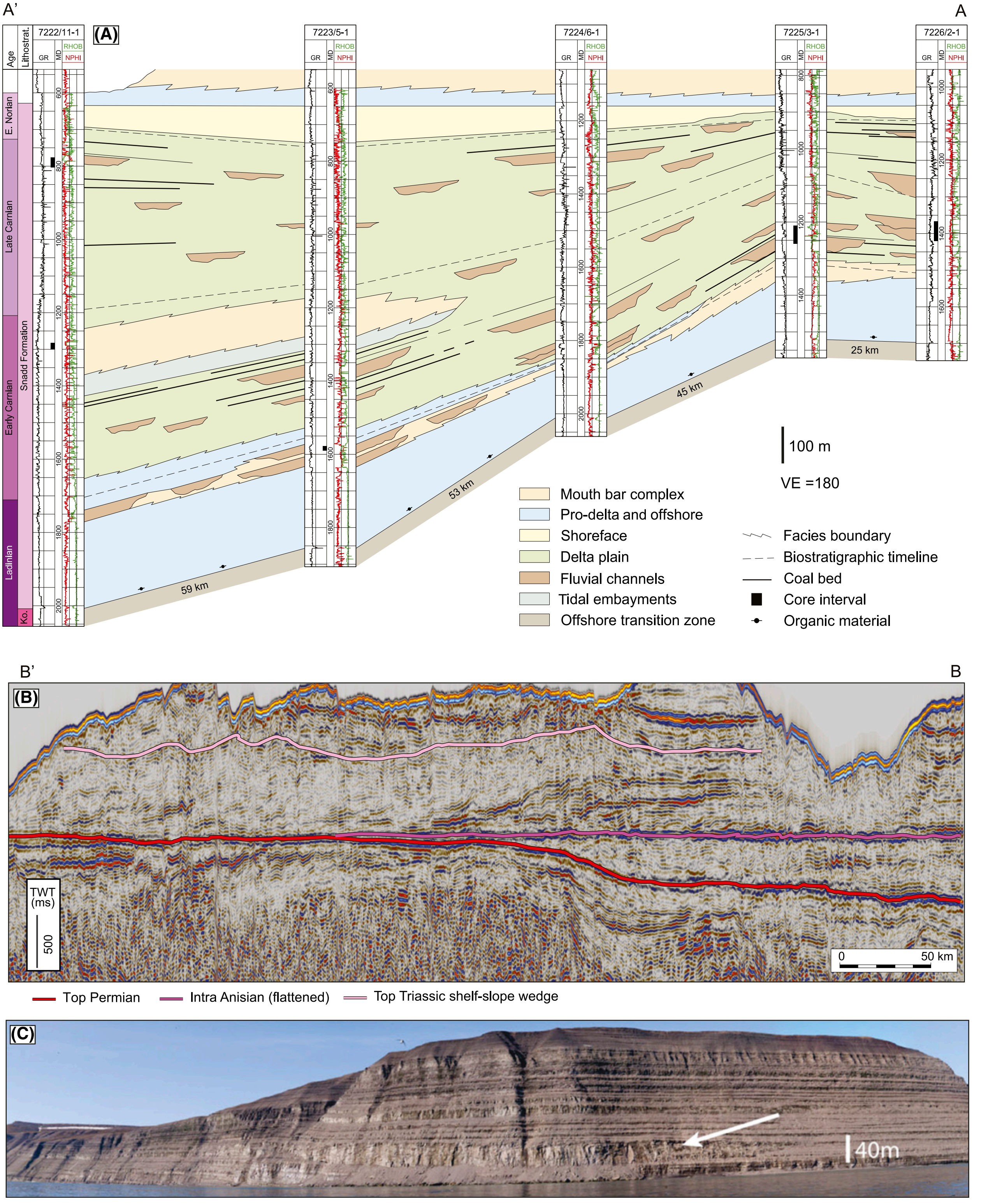

Figure 4. Triassic regression in the Barents Sea. (A) Well correlation showing Triassic regression from the east and Carnian transition from marine to continental conditions. (B) Seismic reflection line showing the northernmost termination of the Upper Triassic shelf–slope wedge system east of Svalbard. (C) Outcrop photograph showing erosive Carnian–Norian fluvial channel (arrow) on Hopen southeast of Svalbard (photograph courtesy of Tore Grane Klausen). These observations suggest that marine accommodation was not filled until the latest part of the Triassic and it is therefore unlikely that sediments from the Barents Sea bypassed to the paleo-Pacific margin. See Figures 1 and 3 for locations.

Fleming et al. (2016) suggests a gradual transition from a Uralian to a Baltic sediment source during the Norian. This pattern may reflect uplift of Baltica and gradual shut-off of the Uralian sediment fairway during Late Triassic uplift of Novaya Zemlya (Figure 3) (Toro et al., 2016). Seismic data also suggest that intrabasin highs acted as local sediment source areas during the Triassic (e.g., Glørstad-Clark et al., 2010). The apparent asymmetry in sediment input between the Barents Sea on one side of the Polar Urals and the West Siberia Basin, Yamal, and Yenisei–Khatanga Basin on the other, may reflect asymmetric topography along the mountain belt.

Biostratigraphic data suggest that the Sverdrup Basin was in communication with the North Slope of Alaska in the Triassic (Mickey et al., 2002). A narrow seaway may have connected the areas across an underlying structural transfer zone (Embry, 1991; Gottlieb et al., 2014). Overall regression also dominated the Sverdrup Basin (Figure 2), and multiple sediment entry points on the northern and southern side of the basin have been recognized based on facies trends in outcropping Triassic strata (Figure 5) (Embry, 1993b; Embry and Beauchamp, 2008). This is also supported by temporal and spatial changes in detrital zircon age distributions and combined zircon and Hf isotope data, indicating sediment sources in the Arctic Canada, the Polar Urals and Taimyr region, and from a land area to the north of the Sverdrup Basin (Figure 3) (Patchett et al., 2004; Omma et al., 2011; Anfinson et al., 2016; Midwinter et al., 2016). This northern provenance area, which also was inferred from progradation directions in outcrop data, is referred to as the Alaska–Chukotka microcontinent (ACMC), or Crockerland (Embry, 1993a). Detrital zircon data suggest that the ACMC delivered both Devonian zircons, which can be linked to the Ellesmerian orogeny (Anfinson et al., 2012), and Permian–Triassic zircons, which are inferred to reflect an episode of magmatism within the ACMC (Ledneva et al., 2011; Midwinter et al., 2016).

Chukotka was situated on the outboard margin of the ACMC toward the paleo-Pacific (Figure 3). Outcropping Triassic rocks document an upward transition from deep-water shales and gravity flow deposits to shallow-marine sandstones sourced from the ACMC (Figure 2) (Bondarenko et al., 2003; Tuchkova et al., 2009). Analysis of regional facies and thickness trends, sandstone petrography, and detrital zircon age distributions suggest that sediments delivered to the South Anyui ocean from the ACMC are different from those sourced from the central Asian fold belt (Prokopiev et al., 2008; Tuchkova et al., 2011). Similar to the Sverdrup Basin, this suggests that the South Anyui ocean received sediment from several source areas.

On the North Slope, Triassic fine- to medium-grained shallow-marine sandstones and are overlain by alluvial conglomerates (Melvin and Knight, 1984; Tye et al., 1999), having detrital zircon signatures indicative of Laurentian provenance (Gottlieb et al., 2014). Approximately 1 km (~0.6 mi) of lithic-rich and texturally immature deep-water Triassic sandstones and shales also crop out on Wrangel Island (Miller et al., 2010). In addition, fine-grained Triassic sandstones crop out in the Lisburne Hills, where they have been interpreted as distal shelfal deposits (Moore et al., 2002). Detrital zircon data from these sands show Neoproterozoic, Paleozoic, and Permian–Triassic age distributions typical of rocks found in the Polar Urals and Taimyr (Miller et al., 2006; Toro et al., 2016; Zhang et al., 2016).

The regional distribution of Paleozoic and Permian–Triassic zircons in Franz Josef Land, the New Siberian Islands, Chukotka, Wrangel Island, Lisburne Hills, and Sverdrup Basin has led to the common interpretation that these sediments were all sourced from the Polar Urals and Taimyr (Miller et al., 2006; Omma et al., 2011; Amato et al., 2015; Soloviev et al., 2015; Anfinson et al., 2016), suggesting that these areas were linked through a trans-Arctic Triassic river system (short-hashed routing system in Figure 3) (e.g., Miller et al., 2013; Anfinson et al., 2016). An alternative scenario is that the ACMC itself contained zircons of similar age (Midwinter et al., 2016), so that the dispersed occurrences of Paleozoic and Permian–Triassic zircons can be explained by local drainage originating within the ACMC. In this scenario, the Hanna trough and Wrangel Island areas were situated adjacent to the paleo-Pacific margin, receiving sediment directly from the ACMC, whereas North Slope received sediments mainly from Arctic Canada (Figure 3) (Gottlieb et al., 2014).

EARLY TO MIDDLE JURASSIC

The Early to Middle Jurassic was characterized by transgression and basin widening (Figures 2, 6). The

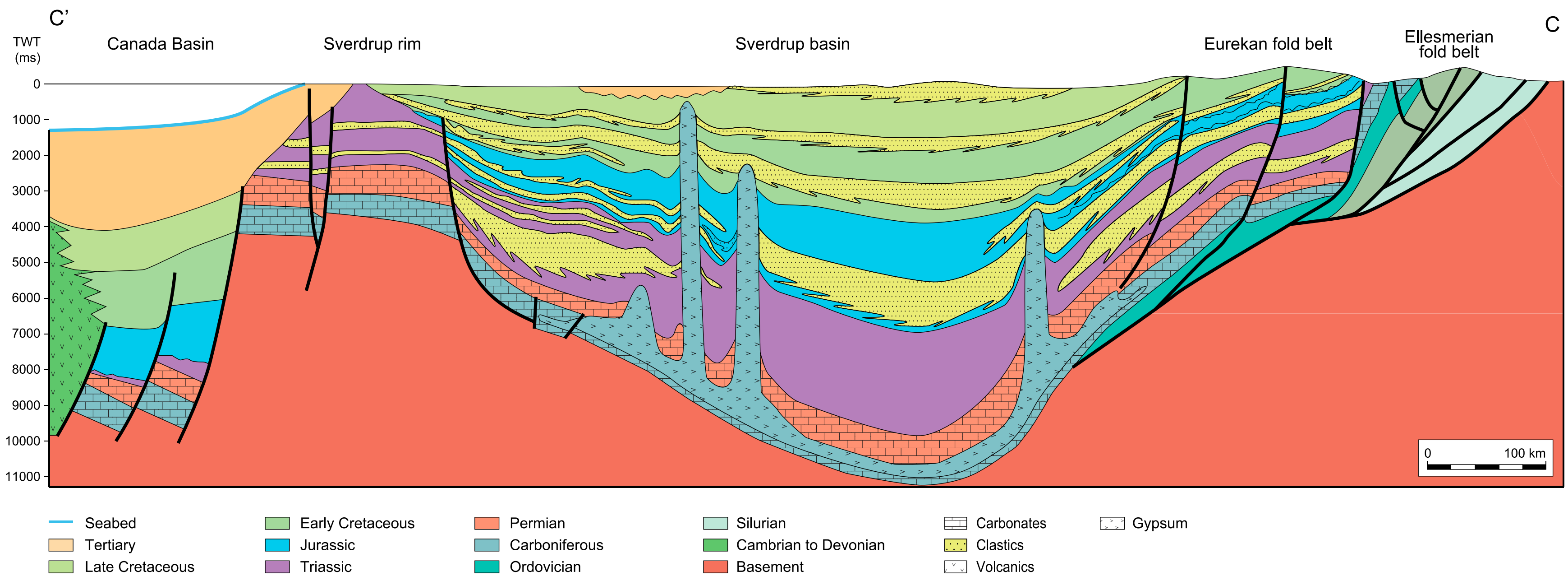

Figure 5. Simplified stratigraphic cross section through the Sverdrup Basin showing clastic wedges sourced from the southeast and northwest. Early to Middle Jurassic rifting along the Canada Basin margin formed the Sverdrup rim topographic high, which separated the main Sverdrup Basin from the Canada Basin. See Figures 1 and 3 for approximate line location. Modified from Meneley et al. (1975) and Stephenson et al. (1987).

Figure 6. The Early to Middle Jurassic was dominated by gradual transgression in most basins. Early rifting commenced in the Canada Basin and accretion along the Pacific margin resulted in sediment delivery into the Hanna trough toward the end of the period. ACMC = Alaska–Chukotka microcontinent; BA = Barrow arch; NSI = New Siberian Islands; WI = Wrangel Island.

period was a time of tectonic quiescence in the South Kara, West Siberia, and Yenisei–Khatanga Basins. The West Siberia Basin experienced gradual transgression (Figure 2) and the shallow (<100 m [<330 ft]), low-gradient basin resulted in large lateral facies shifts during periods of alternating transgressions and regressions (Vyssotski et al., 2006; Kontorovich et al., 2013). The central Asian fold belt, the Polar Urals and the Taimyr areas continued to deliver sediment to local basins (Le Heron et al., 2008; Davies et al., 2010; Zhang et al., 2016), but overall, the rate of subsidence outpaced the rate of sediment input. In the Triassic, the northwestern part of the West Siberia Basin was probably connected to the open ocean though the Yenisei–Khatanga Basin, but in the Early Jurassic, a marine connection may also have been established through the North Kara Basin (Figure 6). Transgression also dominated the Yenisei–Khatanga Basin and the Lena–Anabar area, where Lower and Middle Triassic shallow and marginal-marine deposits are overlain by Upper Triassic and Lower Jurassic shelfal mudstones (Figure 2) (Egorov and Mørk, 2000). Initial subduction took place along the East Siberian craton, where the Kolyma–Omolon microcontinent and several small crustal fragments and island arcs approached from the Pacific (Nokleberg et al., 2001; Shephard et al., 2013). However, the passive margin along the East Siberia craton was still dominated by deposition of shallow and deep-marine clastics (Figure 2) that were sourced from the central Asian fold belt (Oxman, 2003; Prokopiev et al., 2008; Konstantinovsky and Lipchanskaya, 2011).

In the western Barents Sea and Svalbard, Triassic regression was followed by Early Jurassic subaerial exposure and rerouting of sediments toward the southeast (Figure 6) (Faleide et al., 1993). Major flooding and regional transgression of the low-lying Svalbard and western Barents Sea shelves occurred in the Bathonian–Callovian (Figure 2) (Dypvik et al., 2002; Henriksen et al., 2011). Detrital zircon data suggest that sediments mainly were derived from Baltica during this period (Bue and Andresen, 2014; Fleming et al., 2016; Klausen et al., 2017), indicating that the Polar Urals stopped delivering sediments to the western part of the Barents Sea as the basin was transgressed. Similarly, well data suggest that regional flooding resulted in submarine conditions in the eastern part of the Barents Sea during the Callovian; on Franz Josef Land, outcropping Jurassic strata further suggest fully marine conditions in the Aalenian (Dibner, 1998).

A very similar development is also recorded in the Sverdrup Basin, where Triassic and lowermost Jurassic shallow-marine and continental deposits are overlain by transgressive shallow-marine sandstones and shales (Figure 2) (Embry and Beauchamp, 2008). Although the region underwent overall transgression, sands were supplied to the basin margins (Figure 5). At the border to the ACMC, rift-related topography formed in response to incipient extension in the proto-Canada Basin (Figure 5) (Harrison and Brent, 2005; Embry, 2009). Facies relationships and biostratigraphic data suggest that rift initiation outboard of the Sverdrup Basin may have started as early as the Early Jurassic (Mickey et al., 2002; Hadlari et al., 2016). This phase of initial rifting may have been a result of back-arc extension related to early subduction along the paleo-Pacific margin (Kuzmichev, 2009). On Banks Island, Upper Jurassic strata unconformably overlie Devonian rocks, but Sinemurian synrift deposits along the proto-Canada Basin rift system suggest Early Jurassic rift initiation (Dixon, 1982; Embry and Dixon, 1994; Mickey et al., 2002; Grantz et al., 2011). Seismic reflection data collected offshore of Banks Island show synrift depositional wedges documenting initial extension along the Canada Basin (Figure 7). The rift extended further toward the paleo-Pacific and the Mackenzie Delta area, where flanking uplift caused subaerial exposure of the Barrow arch. This early rift episode is also recognized in the detrital zircon data. Lower Jurassic rocks in the Sverdrup Basin lack the late Paleozoic age peak, which is characteristic of the underlying Triassic units, suggesting that the sediment supply from the ACMC was cut off from the Sverdrup Basin during the Early Jurassic, and that Arctic Canada continued as the dominant sediment source (Patchett et al., 2004; Midwinter et al., 2016). Seismic reflection data from the East Siberian shelf suggest that incipient back-arc–related rifting may also have affected the internal part of the ACMC (Bondarenko et al., 2003). But the occurrence of Jurassic marine to marginal-marine strata on the New Siberian Islands (Kos'ko and Korago, 2009) and continued sediment supply to the Hanna trough (Sherwood et al., 2002) suggest that at least parts of

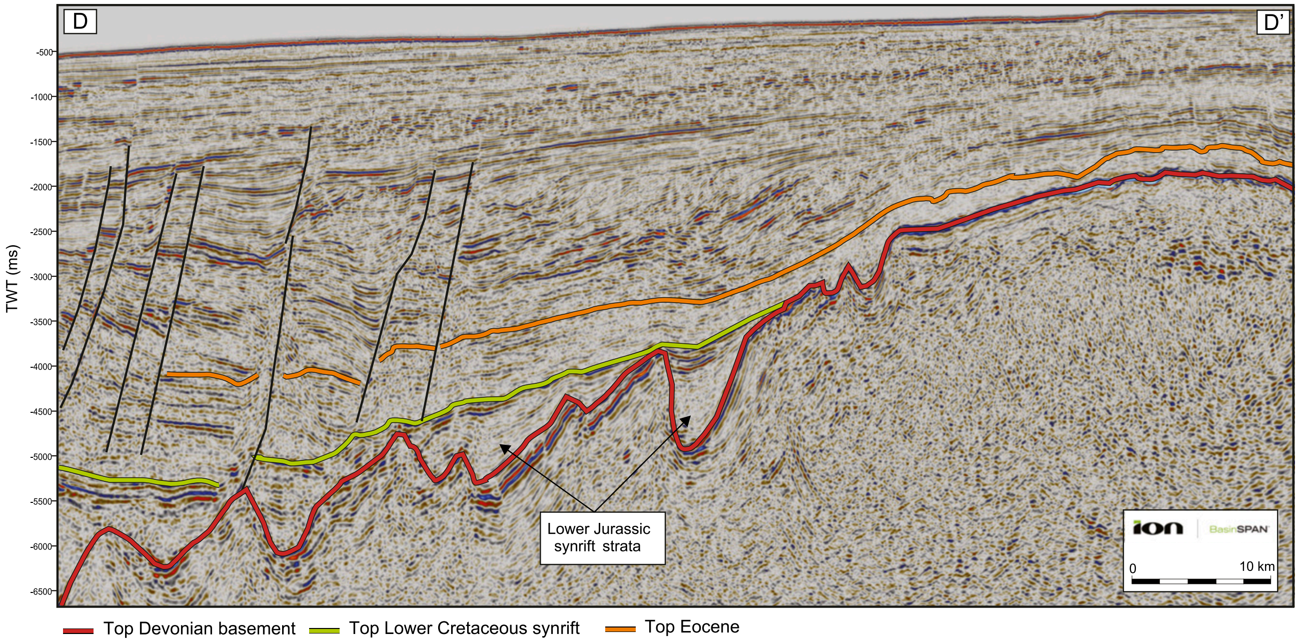

Figure 7. Seismic reflection line offshore Banks Island showing Jurassic and Lower Cretaceous synrift strata unconformably overlaying Devonian prerift clastics below the basement reflector. Synrift strata document the earliest phase of rifting in the Canada Basin as the Alaska–Chukotka microcontinent rotates away from Arctic Canada. The region was dominated by backstepping and low sediment input until the latest Cretaceous–earliest Paleogene. Note major aggradation and progradation above the Eocene reflector documenting a major increase in sediment supply to the margin. See Figures 1 and 6 for line location.

the Triassic topography persisted into the Jurassic (Figure 6).

Subduction along the northern margin of Pangea resulted in the arrival and subsequent collision of several island arcs and exotic terranes during the Mesozoic (e.g., Shephard et al., 2013). Initial collision between the Koyukuk arc (Moore et al., 1994; Nokleberg et al., 2001) and the North Slope passive margin may have started as early as the Middle Jurassic, based on prograding shelf–slope wedges sourced from early compressional topography (Figure 8). A Middle Jurassic onset of the Brookian orogeny was also suggested by Toro et al., (2016). The Hanna trough may thus have received sediments from topographic highs on the ACMC and from the newly formed Brookian topography on the Pacific side (Figure 6).

LATE JURASSIC

The transgression that caused expansion of many Arctic basins during the Early to Middle Jurassic continued into the Late Jurassic (Figures 2, 9). In West Siberia and South Kara basins, the Late Jurassic was characterized by continued subsidence and rapid deepening with water depths of up to 400–800 m (1300–2600 ft) in the central parts of the basin (Kontorovich et al., 2013, 14). Along the basin axis, Lower to Middle Jurassic shallow to marginal-marine deposits are overlain by thick Upper Jurassic organic-rich shales (Vyssotski et al., 2006). It is unclear whether the South Kara and North Kara Basins were in communication at the time, but diachronous development of organic-rich shales (Leith et al., 1993) may suggest that water circulation in the West Siberia and South Kara Basins were somewhat disconnected from the North Kara Basin and the Barents Sea on the far side of Novaya Zemlya. But still a shallow seaway connected the West Siberia Basin to the South Anyui ocean through the Yenisei–Khatanga Basin. Detrital zircon data from Upper Jurassic rocks on the southern flank of the Taimyr fold belt suggest that the provenance areas for these sediments were dominated by rocks related to the Siberian Traps, and the sediments were probably sourced from the East Siberian craton (Zhang et al., 2016). The opposite margin of the East

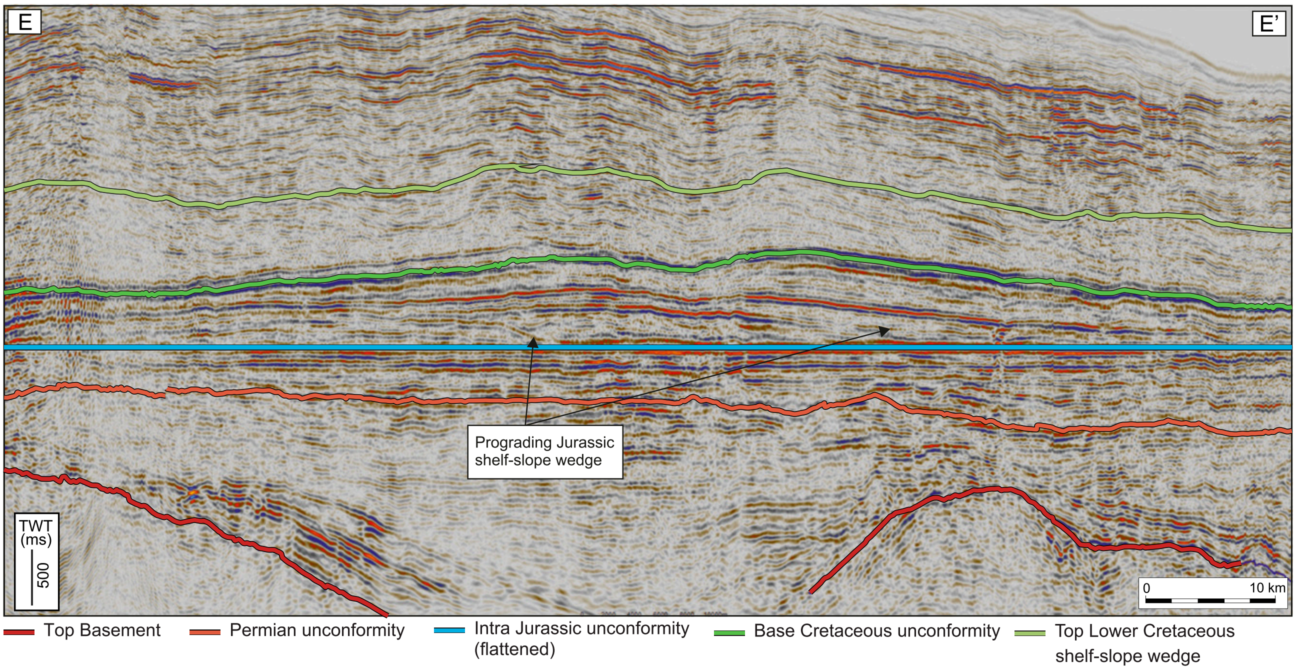

Figure 8. Seismic reflection line showing a progradational Jurassic shelf–slope wedge in the Hanna trough downlapping the flattened intra-Jurassic unconformity. This unit is interpreted as the first phase of sediment delivery from the emerging highland (early Brooks Range) along the paleo-Pacific margin in the northeast. Note also downlapping reflectors between the base Cretaceous unconformity and the top Lower Cretaceous shelf–slope wedge. This unit marks a period of increased sediment supply following closure of the South Anyui ocean and was probably sourced from Chukotka. See Figures 1 and 6 for line location.

Siberian craton (proto-Verkhoyansk fold belt) was still a passive margin sourced from the central Asian fold belt (Figure 9) (Prokopiev et al., 2008), but the approaching and accreting Kolyma–Omolon terrane caused basin shallowing and widespread deposition of deep to shallow-marine sediments along strike of the margin (Figure 2) (Khudoley and Prokopiev, 2007).

Closure of the South Anyui ocean was probably linked to subduction along the paleo-Pacific margin and time-equivalent back-arc extension in the Canada Basin (e.g., Lundin and Doré, 2017), but the exact timing of closure is debated (Kuzmichev, 2009). Collision of the Kolyma–Omolon terrane introduced new sediment source areas to the South Anyui ocean as the basin gradually narrowed. Deformed Oxfordian to Valanginian volcanic-rich, shallow and deep-marine sedimentary rocks on the New Siberian Islands and on Chukotka (Figure 2) suggest diachronous closure along strike (Kyzs'michev et al., 2006; Amato et al., 2015). Deep-water sandstones outcropping on Chukotka have zircon ages consistent with provenance from areas in the Kolyma–Omolon terrane and the East Siberian craton, suggesting that the South Anyui ocean must have been relatively narrow by the Tithonian to allow sediment bypass from the north (Bondarenko et al., 2003; Miller et al., 2008; Harris et al., 2013).

Rifting along the proto-Canada Basin continued and reached climax in the Late Jurassic from the Mackenzie Delta area near the paleo-Pacific margin to the area between Svalbard and Ellesmere Island (Figure 9) (Dixon and Dietrich, 1990). Counterclockwise rotation of the ACMC probably resulted in along-strike variability in extension and subsidence rates, increasing away from the rotation pole in the Mackenzie Delta area. This probably affected synrift stratigraphy within the individual rift segments. Early basin geometry and communication along this extensive (~2000 km [~1200 mi]) long rift system and the adjacent North Slope, Sverdrup, and Barents Sea Basins are poorly constrained, but regional development of time-equivalent, organic-rich shales (Leith et al., 1993) may indicate connection between these basins. Incipient rifting in the Canada Basin was also associated with dextral shear along the (present day) Alpha–Mendeleev margin (Figure 1), which at

Figure 9. The Late Jurassic was dominated by continuous transgression and basin widening. Continued sediment delivery to the North Slope and Hanna trough from the east and rifting within the Alaska–Chukotka microcontinent. Early accretion along the East Siberian shelf formed new provenance areas for sediment delivered to the South Anyui ocean. FJL = Franz Josef Land; NSI = New Siberian Islands; WI = Wrangel Island.

the time was positioned close to Svalbard and Franz Josef Land. The Alpha–Mendeleev ridge is thus inferred to be partly continental (Lebedeva-Ivanova et al., 2006; Døssing et al., 2013; Nikishin et al., 2017), with later volcanic overprint (e.g., Bruvoll et al., 2012), although the complete nature of the ridge is disputed. The terminal transform to the Canada Basin predated the development of the Khatanga–Bering transform (Doré et al., 2015).

Continued compression along the Brooks Range was associated with crustal loading and development of a foreland basin in the North Slope area that was sourced from the growing mountain belt (Figure 9) (Bird and Molenaar, 1992). The foreland basin was confined between the Brooks Range on the Pacific side and the uplifted Barrow arch to the south, which was an emerged high on the flank of the proto-Canada rift basin. Rifting also continued within the ACMC (Bondarenko et al., 2003), splitting the landmass into smaller fragments. One of these blocks formed the Chukchi Borderland (Figure 9) and during opening of the Canada Basin this block rotated clockwise relative to the ACMC (Grantz et al., 2011; Doré et al., 2015).

Late Jurassic deposition in the Sverdrup Basin was dominated by an Oxfordian phase of transgression followed by latest Jurassic–earliest Cretaceous regression of clastic wedges from Arctic Canada and the Sverdrup rim (Figures 2, 5) (Patchett et al., 2004; Embry and Beauchamp, 2008; Omma et al., 2011). The early transgressive phase also expanded the basin to the east and into the Banks Island area (Embry, 1991). At the same time, the Svalbard area experienced deep-water conditions, reaching maximum flooding at the end of the Jurassic (Figure 9) (Dypvik et al., 2002). The western Barents Sea underwent a Late Jurassic rift phase where the central basins were dominated by marine shales (Figure 2) (Faleide et al., 1993). Similar conditions also existed on Franz Josef Land (Dibner, 1998) and elsewhere in the eastern Barents Sea (Petrov et al., 2008). Collectively, these observations suggest that the entire Barents Sea region was covered by a relatively deep (200–300 m [650–980 ft]) intracratonic ocean at the time.

EARLY CRETACEOUS

The Early Cretaceous was characterized by major plate tectonic changes associated with the opening of the Canada Basin and closure of the South Anyui ocean (Doré et al., 2015), resulting in fundamental changes in sediment routing in the Arctic region (Figure 10). Late Jurassic deep-water conditions in the West Siberia Basin were succeeded by regression and transition from underfilled to overfilled conditions (Figures 2, 11). Although minor shelf–slope wedges developed along the Polar Urals, Novaya Zemlya, and Taimyr margins, regional mapping of progradational units show that the dominant sediment source area was the greater central Asian fold belt in the southeast, resulting in more than 500 km (>310 mi) of regression into the basin (Figure 10) (Pinous et al., 2001; Kontorovich et al., 2014). A topographic highland within the central Asian fold belt is supported by fission track thermochronology data showing that this area experienced cooling and probably uplift in the Late Jurassic and Cretaceous in response to the closure of the Mongol–Okhotsk Sea (e.g., Glorie and De Grave, 2016). The total thickness of the regressive wedge in the West Siberia Basin is up to 700 m (2300 ft), comprising 16 stacked, high-frequency transgressive–regressive cycles (Figure 11) (Pinous et al., 2001). Maximum regression was reached during the Aptian and was followed by gradual backstepping and aggradation during the Late Cretaceous (Figure 2) (Kontorovich et al., 2014).

Uppermost Jurassic and Lower Cretaceous marine deposits cropping out in the pre-Verkhoyansk foreland and within the South Anyui suture zone (SASZ) were deposited during the diachronous closure of the ocean between the East Siberian craton, the Kolyma–Omolon terrane, and the ACMC, respectively (Figure 10) (Bondarenko et al., 2003; Miller and Verzhbitsky, 2009; Ershova et al., 2010). Along the SASZ in Chukotka, syntectonic shallow and deep-marine strata range in age from Late Jurassic to Valanginian–Hauterivian (Miller and Verzhbitsky, 2009), and the SASZ itself is crossed by volcanic belts, which suggest Aptian as absolute latest closure age in this area (see discussion in Amato et al., 2015). Cretaceous rocks in the Verkhoyansk fold belt include clastics and volcanics of Early and Late Cretaceous age, consistent with continued accretion of volcanic arcs along the subduction margin (Oxman, 2003; Khudoley and Prokopiev, 2007). Berriasian to lower Valanginian rocks in the Lena–Anabar area also indicate marine conditions, but these are abruptly overlain by upper Valanginian fluvial deposits, which accumulated during

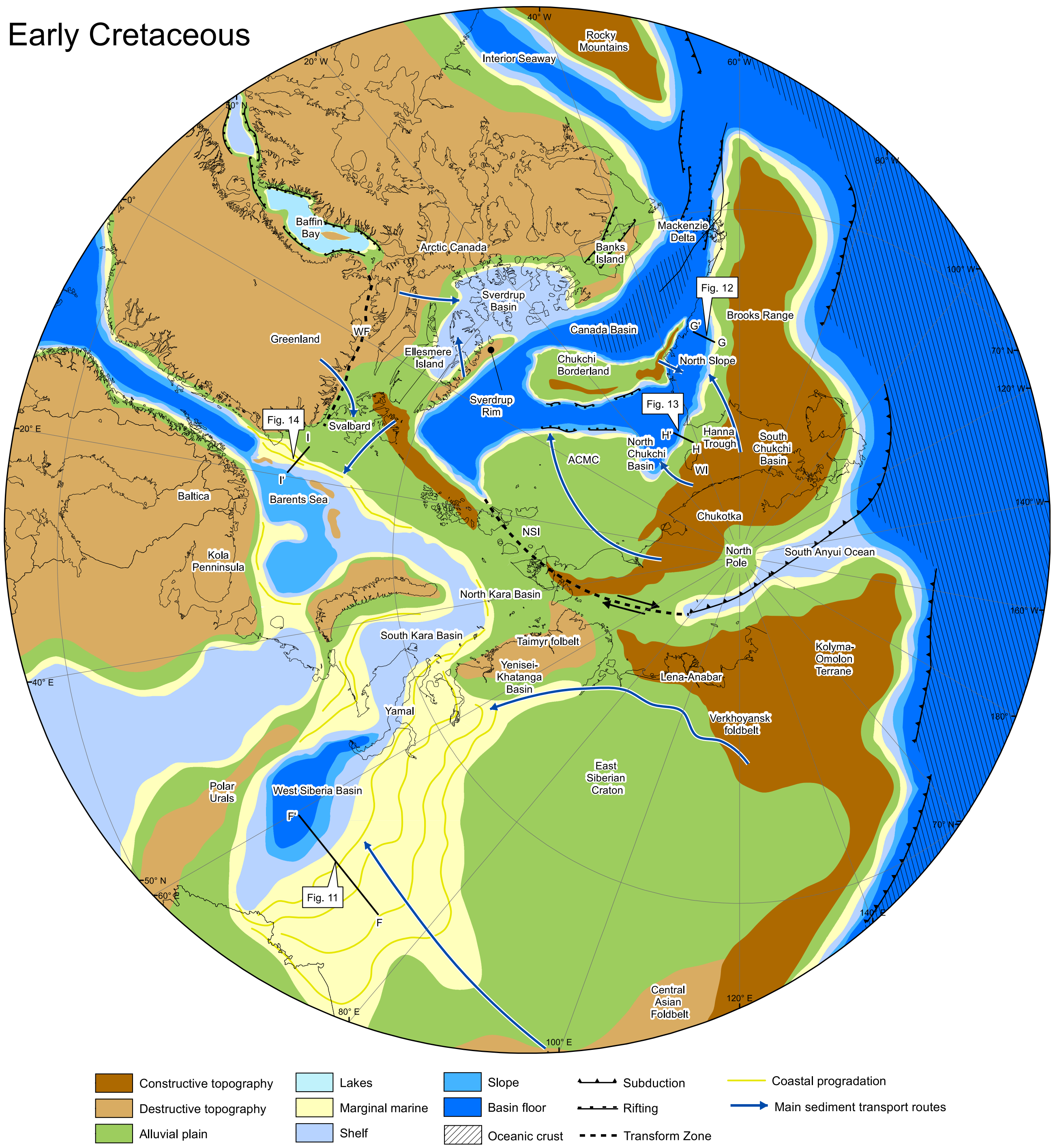

Figure 10. The Early Cretaceous was characterized by a major change in provenance areas and sediment routing. The West Siberia Basin was dominated by regression from the central Asian fold belt and closure of the South Anyui ocean resulted in a continuous mountain belt from Laptev to Banks Island, shedding large volumes of sediment to the northern margin of the Canada Basin. The northern Svalbard–Franz Josef Land margin underwent transient uplift causing southward regression into the Barents Sea. ACMC = Alaska–Chukotka micro-continent; NSI = New Siberian Islands; ; WF = Wegener Fault; WI = Wrangel Island.

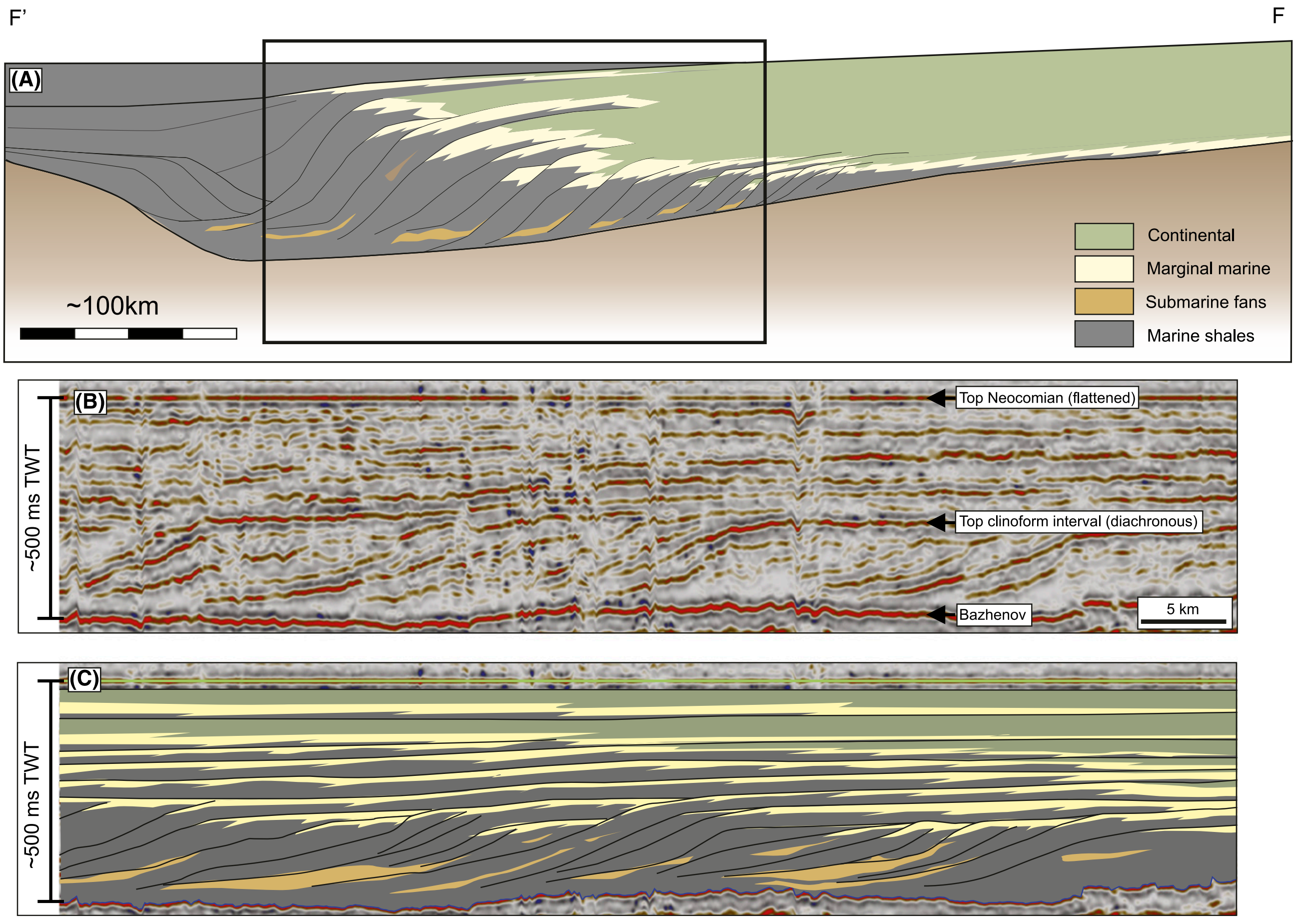

Figure 11. (A) Cartoon showing asymmetric Early Cretaceous regression in the West Siberia Basin. Seismic mapping show that the sediments mainly were derived from the central Asian fold belt. Uninterpreted (B) and interpreted (C) seismic inset line showing stacked transgressive–regressive shelf–slope wedges fronted by submarine fans. The basin underwent rapid subsidence at the time and the water depth in the central part of the basin was probably several hundred meters. See Figures 1 and 10 for line location.

the final transition from marine to continental conditions and closure of the South Anyui ocean along the SASZ (Ershova et al., 2010). The inferred absence of Lower Cretaceous deposits in the Laptev Sea (Figure 2) (e.g., Drachev et al., 1998) may indicate that the Laptev area was subaerially exposed at the time (Figure 10), or that erosional material originating from the Verkhoyansk fold belt was trapped locally in the foreland basin. Aptian–Albian continental clastics on the New Siberian Islands are overlain by volcanic rocks believed to be associated with the SASZ to the north (Kos'ko and Trufanov, 2002). Deformation of, and unconformities within, Upper Jurassic and Lower Cretaceous strata on the eastern margin of Taimyr and in the Lena–Anabar area suggest that these regions also were affected by inversion related to closure of the South Anyui ocean (Verzhbitsky and Khudoley, 2010). The Yenisey–Khatanga Basin area remained dominantly marine until the Barremian (Kontorovich et al., 2014), when the basin was filled by progradational clastic wedges from the northeast (Figure 2). Building this scenario, it is possible that the late pulse of clastic material that was introduced to the Yenisei–Khatanga Basin and the northeastern parts of the West Siberia Basin reflects the final closure of the South Anyui ocean, overfilling of the pre-Verkhoyansk foreland basin and rerouting of the clastic system toward the southwest (Figure 10). In this model, rivers originating in the Verkhoyansk highlands may have filled the Yenisei–Khatanga Basin during the Barremian, reaching maximum regression in the northeastern part of the West Siberia Basin in the Aptian.

The closure of the South Anyui ocean between 150 and 130 Ma overlaps with the inferred time of sea floor spreading in the Canada Basin, which is believed to have started circa 125 Ma (Doré et al., 2015). If

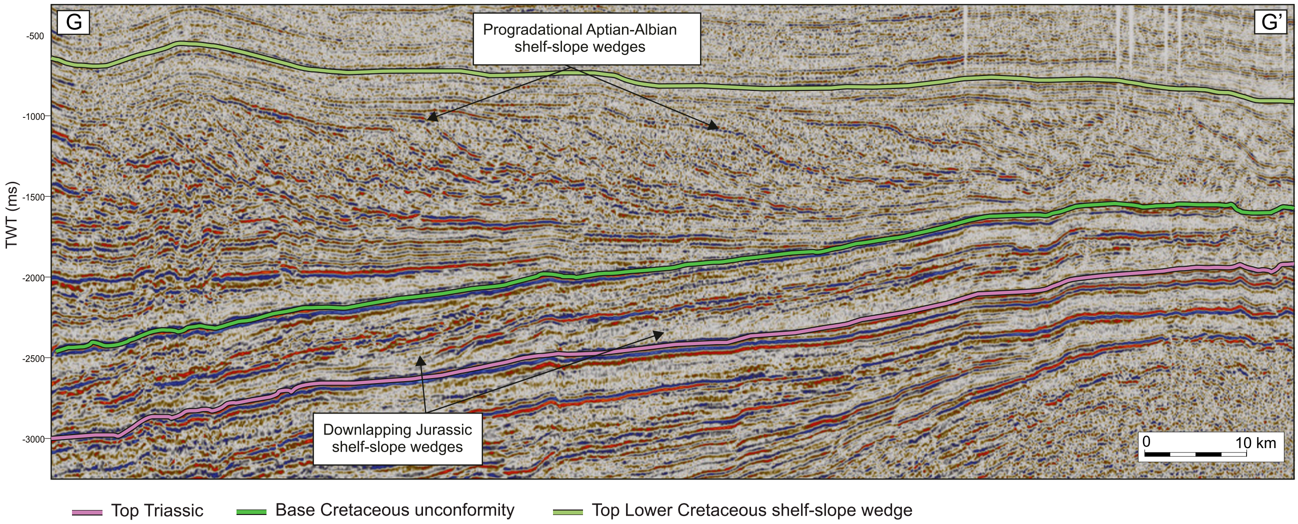

Figure 12. Seismic reflection line across the North Slope foreland basin showing thick, downlapping shelf–slope wedges of Aptian–Albian age above the base Cretaceous unconformity. Detrital zircon and paleocurrent data suggest that the sediments mainly were derived from Chukotka in the northwest. Also note downlapping Jurassic shelf–slope wedges between the top Triassic and base Cretaceous reflectors, indicating sediment dispersal from a different source area at the flank of the early Canada Basin (Barrow arch) or Arctic Canada to the southeast. See Figures 1 and 10 for line location.

sea-floor spreading continued to circa 80 Ma, the last phase of rotational opening of the Canada Basin must have been accommodated by deformation elsewhere, and may have been taken up as lateral movement along the SASZ (Sokolov et al., 2002) or farther inboard of the SASZ.

The early Canada Basin was probably confined with conditions favorable for deposition of organic-rich shales (Lundin and Doré, 2017). Locally sourced synrift deposits are unconformably overlain by marine shales in the lower postrift section (Dixon and Dietrich, 1990). Similar to the North Slope, the Mackenzie Delta region also experienced a major change in provenance area, from a southeastern Laurentian source in the earliest Cretaceous to a northwestern source in the middle Cretaceous (Figure 2) (Dixon et al., 2008). In addition, continued accretion and loading along the northern Rocky Mountains resulted in deepening of the interior seaway foreland basin and connection to the Mackenzie Delta region (Figure 10) (Schröder-Adams, 2014).

In the Brooks Range, subduction along the paleo-Pacific margin continued to add exotic terranes (Shephard et al., 2013). Despite active accretion during the earliest part of the Cretaceous, the North Slope foreland continued to be a relatively deep-water basin (Houseknecht and Bird, 2011), with favorable conditions for accumulation of organic-rich shales in the center (Leith et al., 1993; Peters et al., 2006), and shallow-marine clastics on the basin flanks (Bird and Molenaar, 1992). Detrital zircon data document a change in provenance area from a local source in the Brooks Range in the Late Jurassic to a predominant axial source where sediments were derived from recycled Triassic rocks on Chukotka in the Early Cretaceous (Figure 10) (Moore et al., 2015). Seismic reflection data from the South Chukchi Basin suggest that the area experienced Early Cretaceous deformation (Verzhbitsky et al., 2012), and was probably subaerially exposed at the time. This was followed by a dramatic increase in sediment flux during the Aptian–Albian when 500 km (310 mi) of regression filled the 700–1400-m (2300–4600-ft)-deep North Slope foreland basin (Figures 8, 12) (Bird and Molenaar, 1992; Houseknecht et al., 2009). Paleocurrent data, progradation directions, and detrital zircon data suggest that the main provenance area for the sediment was Chukotka (Bird and Molenaar, 1992; Lease et al., 2014; Moore et al., 2015). This was the last period with sediment input from both the Brooks Range and the exposed northern flank of the Canada Basin; from the Barremian, sediments were only derived from the west (Figure 2).

Hyperextension of continental crust or mantle exhumation took place further north in the North

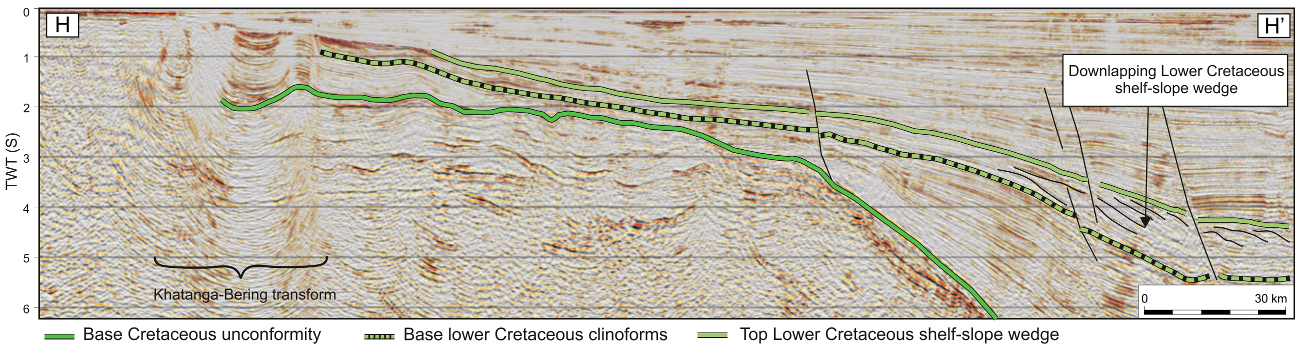

Figure 13. Seismic line crossing the outer North Chukchi Basin margin east of Wrangel Island. The thick (>6 sec) sedimentary succession was deposited during and after rifting of the Chukchi Borderland in response to slow hyperextension or mantle exhumation. Note downlapping shelf–slope wedges between the base and top Lower Cretaceous reflectors. The Lower Cretaceous prograding wedge is inferred to be of Aptian–Albian age. Note also the overlying units, which represents continued Late Cretaceous and Cenozoic regression of a rift-tip delta. The location of the Khatanga–Bering transform is highlighted. Modified from Drachev (2011). See Figures 1 and 10 for line location.

Chukchi Basin, resulting in a very deep outboard basin between the Chukchi Borderland and Wrangel Island (Figure 13). Initially, this basin was probably filled with deep-water sediments, but seismic data suggest that progradation of shelf–slope wedges from the north resulted in an overfilled basin setting in the Early Cretaceous (Drachev, 2011). Although poorly dated, it is inferred that this regressive unit is time-equivalent to the Aptian–Albian system on the North Slope.

The Sverdrup Basin experienced local rifting, volcanism, and overall regression during the Early Cretaceous (Figure 2) (Embry, 1991; Embry and Beauchamp, 2008). Sediments were mainly derived not only from Arctic Canada but also from the Sverdrup rim along the outer rifted margin (Figure 5) (Patchett et al., 2004; Røhr et al., 2010; Tullius et al., 2014). The link between the eastern Sverdrup Basin, northernmost Baffin Bay and the Barents Sea is poorly constrained, but Early Cretaceous rifting and deposition of synrift continental clastics in Baffin Bay may have coincided with shearing along the Wegener fault on the northern margin of Greenland (Figure 10) (Whittaker et al., 1997; Harrison and Brent, 2005; Gregersen et al., 2013), causing local uplift in this region. This initial phase of extension in the Baffin Bay was associated with deposition of synrift clastics in restricted basins sourced from Greenland (Røhr et al., 2008).

On Svalbard, the Lower Cretaceous succession documents regression and sediment delivery from Greenland and an area north of Svalbard (Figure 10) (Steel and Worsley, 1984; Dypvik et al., 2002). South-flowing braided streams transported sediments into the western Barents Sea (Figure 14) (Gjelberg and Steel, 2012), but the prograding shelf–slope wedges never reached the southeasternmost part of the basin (Faleide et al., 1993). The timing of regression and sediment delivery from the north coincides with movement along the Khatanga–Bering transform (Doré et al., 2015), and it is likely that uplift along the outer margin north of Svalbard was a result of regional volcanism and isostatic adjustment to this tectonic event (Gjelberg and Steel, 1995; Midtkandal and Nystuen, 2009). A major phase of cooling and uplift of northern Svalbard is inferred from fission track thermochronology data, suggesting that the area remained high and above base level from the Late Jurassic to the early Paleogene (Dörr et al., 2012). Detrital zircon data also suggest that Greenland was an important source area for sediment being delivered to the northwestern part of the Barents Sea in the Early Cretaceous (Bue and Andresen, 2014). A possible scenario is that this regional uplift north of Svalbard cut off the pre-Cretaceous seaway linking the area to the Sverdrup Basin, so that for the first time since the assembly of Pangea, the Arctic Ocean was separated into an eastern segment that connected to the North Atlantic, and a western segment that linked to the Pacific (Figure 10) (Lundin and Doré, 2017).

Seismic reflection and shallow core data suggest that the Lower Cretaceous regressive clastic wedge also is present in the area between Svalbard and Franz

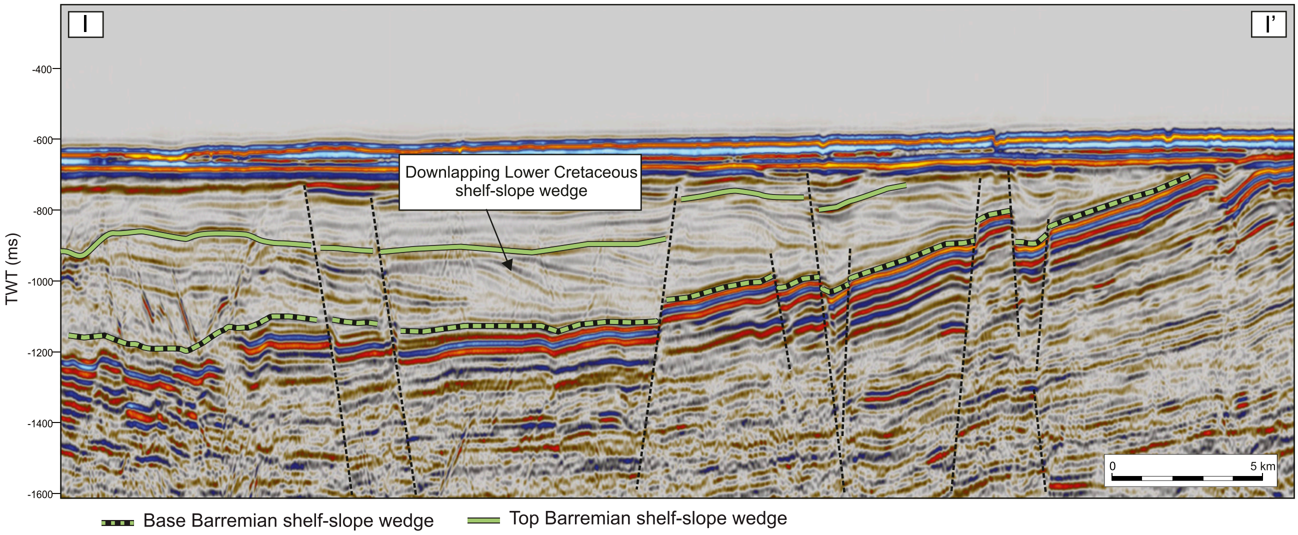

Figure 14. Seismic reflection line showing regressive shelf–slope wedges between base and top Barremian reflectors in the northern Barents Sea. The regression event was driven by dynamic uplift north of Svalbard and covered also the area toward Franz Josef Land. Minor regression also occurred from the east and south. Data acquired by Fugro. See Figures 1 and 10 for line location.

Josef Land (Gustavsen et al., 1997). Further to the northeast, Berriasian to Hauterivian deposits on Franz Josef Land document regression, with continental deposits overlying Upper Jurassic marine shales, followed by Barremian to Albian mixed continental clastics and volcanics (Dibner, 1998). The Barremian to Albian part of the succession is associated with regional unconformities and Dibner (1998) suggests a period of regional uplift north of the present-day islands (Figure 1). Similar to Svalbard, this uplift was likely a result of movement along the distal Canada Basin transform at the eastern margin of the Canada Basin. Seismic reflection and well data from the eastern Barents Sea show Berriasian to Albian regression from Novaya Zemlya in the east and from the Kola Peninsula in the south (Figure 2) (Kaminsky et al., 2011; Kayukova and Suslova, 2015; Marín et al., 2017), indicating that the Barents Sea was dominated by regression from all margins (Figure 10).

LATE CRETACEOUS

Following major Early Cretaceous regression in the West Siberia Basin, transgression and backstepping started in the Albian and regional Cenomanian–Turonian flooding resulted in rapid basin widening and a transition from continental and marginal-marine deposits to shallow-marine and shelfal conditions (Figures 2, 15) (Kontorovich et al., 2014). Despite regional transgression, sediments continued to be delivered to the southern part of the basin from the central Asian fold belt. At the same time, transgression also flooded parts of the Yenisei–Khatanga Basin, although clastics also were sourced from the East Siberian craton and Taimyr. One possible driver for backstepping in the Yenisei–Khatanga Basin is the development of the Ust' Lena rift system, which is the onshore continuation of the proto Laptev rift (Figure 15) (Drachev et al., 1998; Franke et al., 2001). It is possible that this rift event breached the topographic barrier that directed sediment from the Verkhoyansk fold belt into the Yenisei–Khatanga Basin in the Early Cretaceous by creating local rift accommodation. In this scenario, a major axial river system along the pre-Verkhoyansk foreland would have delivered large amounts of sediments to the tip of the rift (Figure 15). This interpretation is supported by seismic reflection data from the Laptev Sea, which documents up to 10 km (6 mi) of Upper Cretaceous to Eocene deposits (Drachev, 2011). The New Siberian Islands were located at the flank of the proto-Laptev rift and outcropping Upper Cretaceous strata suggest continental conditions and high input of volcanic material (Kos'ko and Trufanov, 2002).

Shearing along the Khatanga–Bering transform was initiated along the northern margin of the East Siberian shelf during the Late Cretaceous in response

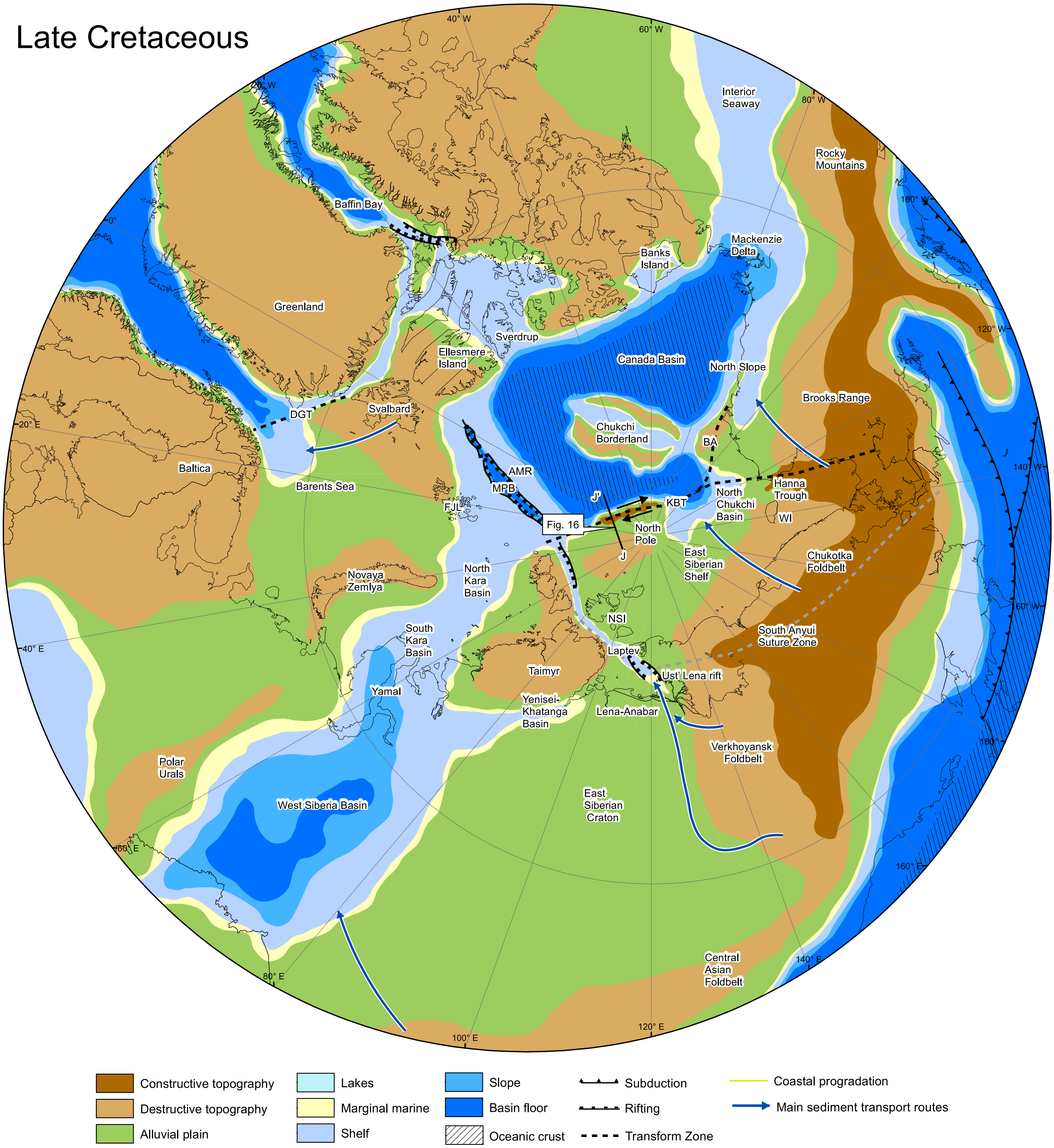

Figure 15. The Late Cretaceous was dominated by regional regression into the northern and western margins of the Canada Basin. The West Siberia Basin underwent transgression and sediments originating from the Verkhoyansk fold belt were rerouted into the proto-Laptev rift. The Barents Sea was mostly subaerial. AMR = Alpha–Mendeleev ridge; BA = Barrow arch; DGT = De Geer transform; FJL = Franz Josef Land; KBT = Khatanga–Bering transform; MPB = Makarov–Podvodnikov Basin; NSI = New Siberian Islands; WI = Wrangel Island.

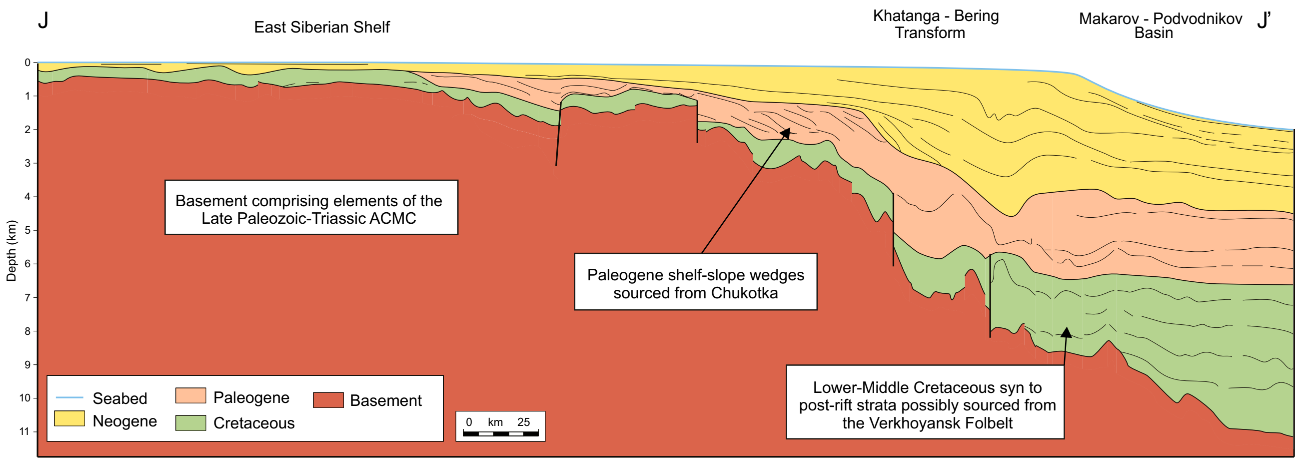

Figure 16. Interpreted seismic section from the East Siberian shelf. The Khatanga–Bering transform influenced basin topography and deposition in the area. Lower Cretaceous strata may be preserved in the distal part of the basin but the section is inferred to be thin or absent on the shelf. The lower part of the Cretaceous section may represent sediment delivery from the Verkhoyansk fold belt prior to opening of the Eurasia Basin. Later, sediments were derived from the eastern part of the Chukchi fold belt. The basement on the East Siberian shelf is inferred to contain late Paleozoic–Triassic volcanics, which were eroded and transported to nearby basins when the area was part of the Alaska–Chukotka microcontinent (ACMC). Modified from Sekretov (2001). See Figures 1 and 15 for line location.

to opening of the Makarov–Podvodnikov Basin southeast of the Alpha–Mendelev ridge (Figure 15) (Doré et al., 2015). Local topographic highs and lows along the shear zone would have directed sediments derived from the SASZ and the Chukotka fold belt into the basin. Seismic reflection data from the East Siberian shelf show an up to 5-km (3-mi)-thick wedge of inferred Upper Cretaceous outer shelf, slope and deep-water deposits (Figure 16) (Sekretov, 2001). This is also supported by fission track data from the Chukotka fold belt, which suggest cooling and exhumation during the middle Cretaceous, consistent with a major unconformity offshore (Figure 2) (Miller and Verzhbitsky, 2009). On the East Siberian shelf and in the North Chukchi Basin, large river systems originating in the Chukotka fold belt are thought to have flowed toward and along foreland basins and topographic lows created during earlier rifting. Most of these basins are probably dominated by fluvial, marginal marine and inner shelf deposits (Drachev et al., 2010).

Propagation of the Brooks Range thrust front resulted in regional uplift of the proximal part of the Hanna trough and North Slope (Bird and Molenaar, 1992; Moore et al., 1994; Sherwood et al., 2002). Except for a Cenomanian–Turonian transgression event, uplift and increased sediment flux continued to drive the clastic wedge into and across the foreland basin (Figures 2, 12) (Houseknecht and Bird, 2011). In the Mackenzie Delta region, amalgamation of island arcs eventually closed the connection with the Pacific (Nokleberg et al., 2001; Shephard et al., 2013), but the basin was still connected to the global ocean through the Interior Seaway to the south (Figure 15). The Cenomanian succession in the Sverdrup Basin is dominated by volcanic material deposited during an episode of uplift along the northern basin margin (Embry and Beauchamp, 2008). This was succeeded a major transgressive event with deposition of shales in the central part of the basin, followed by a renewed phase of Late Cretaceous regression from local sediment sources areas (Figures 2, 5) (Embry, 1991; Ricketts and Stephenson, 1994). Late Cretaceous rifting in the Baffin area caused regional subsidence and transgressive conditions during the Turonian, where marine shales overlie older continental Cretaceous deposits (Whittaker et al., 1997; Harrison et al., 2011; Gregersen et al., 2013).

Absence of Upper Cretaceous strata on Svalbard (Steel and Worsley, 1984; Smelror and Larssen, 2016) indicates that this area remained a topographic high in the Late Cretaceous as a result of early transpression along the De Geer transform (Figure 15) (Håkansson and Pedersen, 2001) and rifting of the Alpha–Mendeleev ridge from the Svalbard–Franz Josef Land margin. The northwestern part of the Barents Sea experienced uplift in the Late

Cretaceous (Riis et al., 1986), and sediments were shed southward into deep-water basins (Figure 2). Further east, the eastern Barents Sea and North Kara Basin also underwent major uplift in the Late Cretaceous (Musatov and Pogrebitskij, 2000).

PALEOGENE

From the Late Cretaceous to the Eocene, the West Siberia Basin was in open communication with the Tethys in the south, with the Laptev area in the east through the Yenisei–Khatanga Basin, and to the North Kara Basin in the north (Figure 17) (Akhmetiev et al., 2012). Minor changes in base level resulted in widespread facies shifts because of the low gradients within the basin, but shallow-marine conditions prevailed in the basin center (Figure 2). Rifting propagated southward in the Laptev Sea as extension in the Makarov–Podvodnikov Basin ended and rifting of the Lomonosov Ridge started during initiation of the Eurasia Basin in the Late Cretaceous (Drachev et al., 2003; Evangelatos and Mosher, 2016). In the same way the paleo-Lena was pinned to the Makarov–Podvodnikov basin during opening, the river continued to supply sediments into the opening Eurasian Basin parallel to the basin axis (Figure 17).

Compression along the Verkhoyansk fold belt came to a halt and was succeeded by postorogenic extension and formation of intraorogenic sedimentary basins (Drachev et al., 2010). Basinward, the Paleogene succession on the New Siberian Islands is dominated by terrestrial clastics and weathering horizons, indicating continental conditions with minor marine intrusions (Kos'ko and Korago, 2009). Along the margin of the East Siberian shelf, large river systems draining the interior fold belts filled all accommodation, resulting in widespread regression from the New Siberian Islands to the North Chukchi Basin (Figures 2, 13, 16) (Sekretov, 2001; Drachev, 2011). This period also represents a prominent phase of movement along the Khatanga–Bering transform (Doré et al., 2015), and it is expected that later deformation had minor influence on deposition in the already overfilled basin.

A similar situation developed in the Hanna trough and North Slope areas. The long-lived and subaerially exposed Barrow arch was probably buried in the earliest Cenozoic, as thick progradational shelf–slope wedges sourced from the Brooks Range prograded toward the outer, deep-water basins (Figures 2, 17) (Houseknecht and Bird, 2011). Along the Pacific margin, the Paleogene marks a shift in subduction style, as long-lived (Early Jurassic–Paleogene) continental accretion of exotic terranes and island arcs along North America and eastern Siberia terminated and subduction jumped seaward forming the present-day Aleutian arch (Shephard et al., 2013). High sediment flux along the margin resulted in significant basinward progradation of shelf–slope wedges along the entire margin from North Slope and Mackenzie Delta to Banks Island (Figures 2, 7, 18), and possibly also further east toward Ellesmere Island. In the Mackenzie Delta region, the open seaway between the Canada Basin and the Interior Seaway closed, rerouting sediments from the Brooks Range to the outer basin margin (Figure 17). The earliest pulse of sediment delivered to the Mackenzie Delta was arrived in the Paleogene (Figure 2), in response to uplift along the Brooks Range (Helwig et al., 2011). The delta continued to prograde into the Canada Basin during the Cenozoic and was periodically subjected to regional compressional folding during the Paleogene–Miocene (Figure 18). The resulting structures severely affected sediment fairways by rerouting sediments between and axially along syncline depocenters. The same folds also affected the super-Miocene stratigraphy by pinning the shelf–slope break and the transition from shallow to deep-water conditions.

Paleogene breakup in the Eurasia Basin was associated with activity along the De Geer transform, which extended from northern Baltica in the east to the western part of the Canadian Arctic Islands in the west (Faleide et al., 2008). In the Sverdrup Basin, early Paleocene transgressive marine shales are overlain by regressive shallow-marine clastics mainly sourced from the southeast (Figure 2) (Ricketts & Stephenson, 1994), marking the last regional phase of deposition before the Eurekan orogeny (Figure 17) (Embry and Beauchamp, 2008). The Paleocene–Eocene Eurekan orogeny was a consequence of the opening of the north Atlantic together with ongoing opening of Baffin Bay, causing northward motion of Greenland and collision with Ellesmere Island (e.g., De Paor et al., 1989; Doré et al., 2015). Fission-track data show that significant uplift occurred in the area around Ellesmere Island during this period (Grist and Zentilli, 2006), forming new

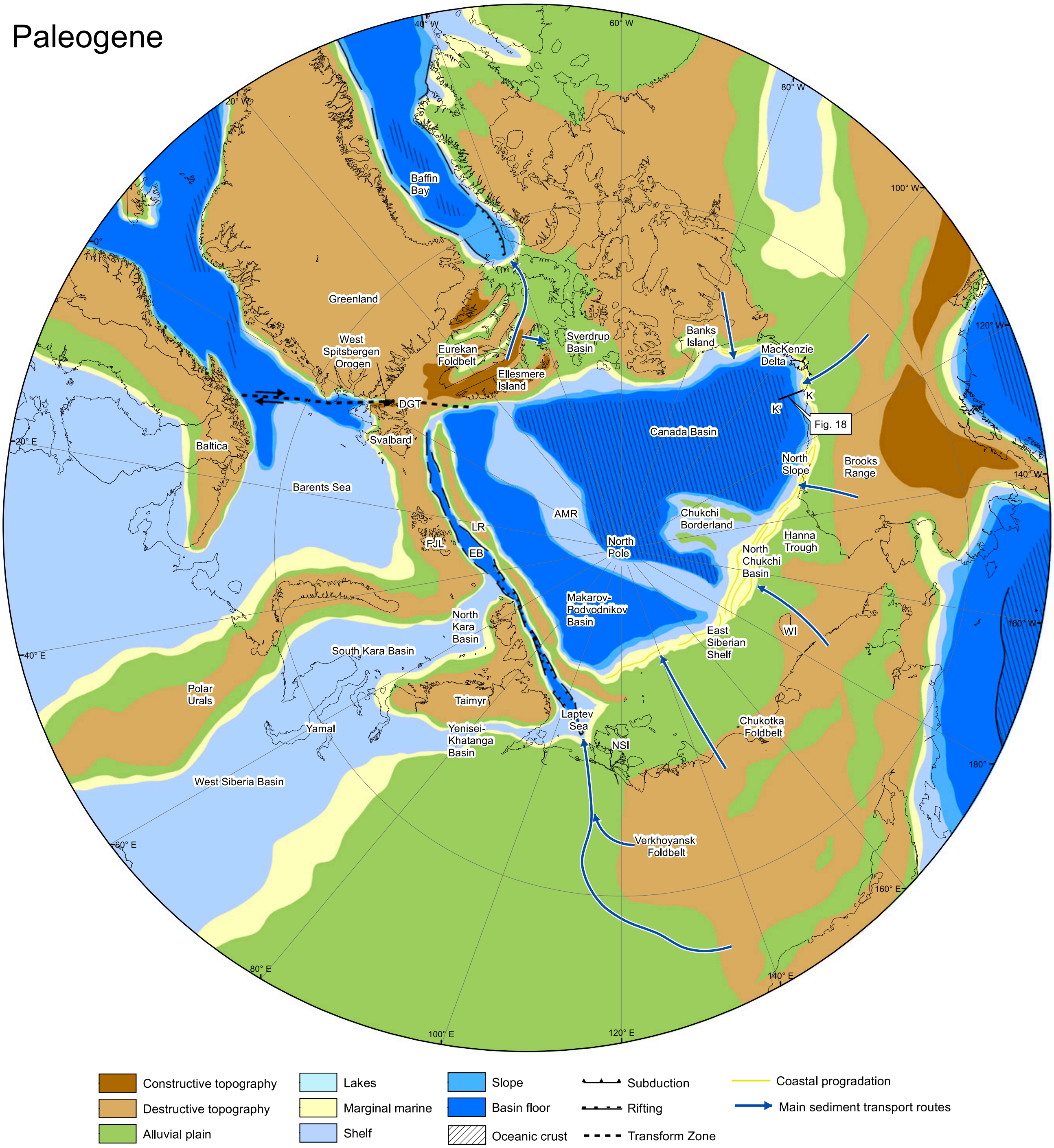

Figure 17. The Paleogene was dominated by major regression into the Canada Basin across the East Siberian shelf, the North Slope, and Mackenzie Delta. Rifting in the Eurasia Basin trapped sediments sourced from the Verkhoyansk fold belt. The Barents Sea and West Siberia Basin underwent transgression and flooding whereas sediments from the Eurekan orogen were routed southward to form a rift-tip delta in the Baffin Bay. AMR = Alpha–Mendeleev ridge; DGT = De Geer transform; EB = Eurasia Basin; FJL = Franz Josef Land; LR = Lomonosov Ridge; NSI = New Siberian Islands; WI = Wrangel Island.

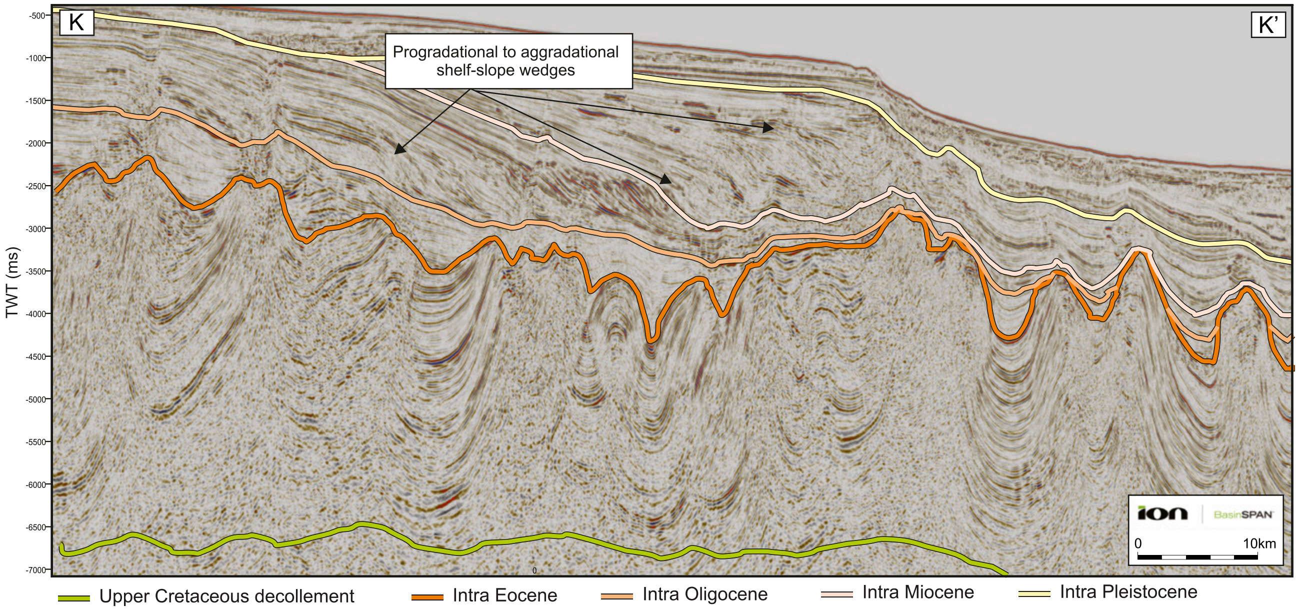

Figure 18. Seismic reflection line from the Mackenzie Delta area showing major Paleogene and Neogene regression and the formation of a rift–tip delta above the deformed Upper Cretaceous succession. See Figures 1 and 17 for line location.

local sediment sources areas for sediments deposited in nearby syntectonic basins (Ricketts and Stephenson, 1994). Simultaneous transpression between Greenland and the western Barents Sea along the De Geer transform resulted in the West Spitsbergen orogeny on Svalbard. Uplift of the western part of Svalbard resulted in high sediment flux to the foreland basin, which is dominated by regressive shelf–slope wedges (Steel and Worsley, 1984). Facies relationships and zircon data suggest that this compressional event also marked a major change in provenance areas, from a northern source area in the Paleocene to a more westerly source during the Eocene (Petersen et al., 2016). Continued extension and Paleogene sea-floor spreading in the Baffin Bay to the south coincided with the Eurekan orogeny in the north, and large volumes of sediment were shed axially southward to produce a large submarine fan in the northern part of Baffin Bay (Harrison et al., 2011; Knutz et al., 2012). The Paleocene was also dominated by magmatic activity on Greenland, Ellesmere Island, and Svalbard, reflecting initial sea-floor spreading in the northern North Atlantic and in the Eurasia Basin (e.g., Berglar et al., 2016). The northeastern tip of Greenland and the northern part of Svalbard were still dominated by erosional hinterland, but relatively deep marine platform conditions prevailed across large parts of the Barents Sea (Figure 17) (Faleide et al., 1993; Setoyama et al., 2011).

IMPLICATIONS FOR SEDIMENT ROUTING AND BASIN FILL

A Triassic Central Arctic Highland?

The presence, extent, and paleotopography of the ACMC landmass in the Triassic is fundamental for predicting sand delivery to underexplored basins such as the East Siberian shelf, North Chukchi Basin, and Hanna trough (Figure 3). In the Triassic, the Hanna trough was located approximately 2000 km (~1200 mi) from Taimyr and the Polar Urals. A trans-Arctic river system as suggested by Miller et al. (2013) would either have had to extend across the Barents Sea and Sverdrup Basin, or find its way across the ACMC. The first scenario requires that the Barents Sea and Sverdrup Basins were completely filled in the Triassic to allow bypass to the paleo-Pacific margin, but maximum regression on Svalbard and Franz Josef Land occurred as late as the Norian (Figure 4A) (Dibner, 1998; Dypvik et al., 2002; Lundschien et al., 2014; Vigran et al., 2014). In the Hanna trough, well data suggest that shallow to marginal-marine deposits already existed at the flank of the basin during the earliest Triassic (Sherwood et al., 2002), at a time when the prograding Triassic shoreline was located relatively close to the Polar Urals and Baltica (Figure 4) (Glørstad-Clark et al., 2010; Kaminsky et al., 2011; Lundschien et al., 2014; Eide et al., 2018). Together, these observations contradict a trans-Arctic feeder system across the Barents Sea.

An alternative scenario that could have brought sediments from the Polar Urals and Taimyr to the Hanna trough area is a regional drainage system that crossed the ACMC (short-dashed routing system in Figure 3) (Miller et al., 2013; Anfinson et al., 2016). Facies trends (Embry and Beauchamp, 2008) and detrital zircon data (Midwinter et al., 2016) suggest that significant amounts of sediment were supplied from the ACMC into the Sverdrup Basin in the Triassic. Similarly, facies trends and petrographic data also suggest that the same area supplied sediment into the South Anyui ocean (Figure 2) (Tuchkova et al., 2009, 2011). Long-lived sediment input to these basins is consistent with a central Arctic provenance area that was dominated by significant topography in the Triassic. A trans-Arctic river system would have had to cross this land area on its way to Wrangel Island and the Hanna trough. Although this model is possible, the preferred scenario is one where sediments dispersal to the Sverdrup Basin, Hanna trough, Wrangel Island, and South Anyui ocean areas came directly from topography within the ACMC. A local source for Triassic sediments on Wrangel Island and the South Anyui ocean would be consistent with the high content of lithic fragments and the overall textural immaturity of the sands in these areas (Tuchkova et al., 2009; Miller et al., 2010), which are quite different from the Triassic sands found in the Barents Sea and Svalbard (Riis et al., 2008).

Facies trends in the Sverdrup Basin have long been used to argue for a central Arctic highland (Embry, 2009), and this scenario has recently been supported by detrital zircon and isotope data (Anfinson et al., 2016; Midwinter et al., 2016; see also Hadlari et al., 2016). The occurrence of late Paleozoic zircons in Triassic sedimentary rocks along the paleo-Pacific margin and in the Sverdrup Basin has been one of the key arguments for trans-Arctic sediment bypass from Taimyr and the Polar Urals (e.g., Miller et al., 2013), but recent dating of late Paleozoic lava flows interbedded with Triassic strata in the Chukotka fold belt (Ledneva et al., 2011) suggest that these may have been locally derived. As a result, and as suggested by Amato et al. (2015) and Midwinter et al. (2016), this may imply that late Paleozoic volcanic rocks are more widespread than previously believed, covering parts of the ACMC in the Triassic. Presently, large parts of the Triassic ACMC landmass are located on the East Siberian shelf (Figure 1). Unpublished seismic reflection data from this area show what has been interpreted as late Paleozoic and Mesozoic basins surrounded by local highs (see figure 9B in Doré et al. 2015). These observations suggest that the basement in this area (Figure 16) may preserve late Paleozoic–Triassic volcanics, which were later eroded from the local highlands. The simplest model is that these deposits were transported locally to nearby basins along the paleo-Pacific margin, the Sverdrup, and the South Anyui ocean areas.

Presence of significant topography on the ACMC has implications for sand delivery to nearby basins during the initial stages of rifting in the Canada Basin. Since the Early to Middle Jurassic was characterized by transgression and flooding of low-lying Late Triassic land areas (Figure 6), there is no potential for trans-Arctic sediment transport at this time (Omma et al., 2011). Remnant Triassic topography on the ACMC could have been a source for synrift sediment on the East Siberian shelf, Hanna trough, and the North Chukchi Basin area at the time (e.g., Sherwood et al., 2002).

The time interval between early rifting and onset of sea-floor spreading in the Canada Basin (from ca. 170 to 125 Ma; Mickey et al., 2002; Doré et al., 2015) overlaps with the inferred closure age of the South Anyui ocean (from ca. 150 to 130 Ma; Miller and Verzhbitsky, 2009; Amato et al., 2015). This overlap has major implications for sediment delivery to the northern margin of the Canada Basin (paleocoordinates) during the rift and early postrift stage. If the South Anyui ocean was an extensive sediment trap on the northern side of the ACMC from the latest Jurassic to the Hauterivian (i.e., foreland basin of Miller et al., 2008), this would limit sediment delivery to the Canada Basin to any remnant topography within the ACMC. If, however, partial closure and uplift of the margin already occurred in the latest Jurassic or earliest Cretaceous, these regions would have formed extensive sediment source areas for these basins.

Early Cretaceous Drainage Reorganization

A major drainage reorganization occurred in the Early Cretaceous (Figure 10), resulting in widespread regression across most of the Arctic (Figure 2). Although most regions were dominated by regression, the timing of initial progradation and the link to the sediment source areas varied across the region. Regression first occurred in the West Siberia Basin where clastic wedges sourced from the central Asian fold belt prograded into the basin from the southeast as early as the Berriasian (Pinous et al., 2001). The next phase of regression occurred in the Hauterivian, when progradation occurred from the southeast into the Sverdrup Basin (Embry, 1991), from the north into Svalbard (Steel and Worsley, 1984) and Franz Josef Land (Dibner, 1998), and from the east into the eastern part of the Barents Sea (Kayukova and Suslova, 2015). The last major phase of regression took place on the North Slope in the late Aptian (Lease et al., 2014), with sediments sourced from land areas to the northwest (Bird and Molenaar, 1992).

This series of regressions can be attributed to a succession of linked plate tectonic events around the Arctic during the Early Cretaceous. Ongoing subduction along the paleo-Pacific margin started with closure of the Mongol–Okhotsk ocean in the latest Jurassic–Early Cretaceous, promoting orogenic uplift (Nokleberg et al., 2001; Glorie and De Grave, 2016) and high sediment input into to the West Siberia Basin. This was followed by closure of the South Anyui ocean and uplift along the Verkhoyansk fold belt. This area may have been the source of a late Hauterivian to Aptian sediment pulse delivered through the Yenisei–Khatanga Basin as deformation in the Laptev area prevented clastics from being shed into the Canada Basin. The implications of this model would be that the Siberian margin of the Canada Basin did not receive sediment from the Verkhoyansk fold belt, but only locally derived clastics from the collisional part of the ACMC (Figure 10). The Cretaceous succession along this margin (Figure 16) may therefore comprise both synrift and early postrift clastics locally shed from the ACMC.

A review of published magmatic ages suggests that subduction of the South Anyui ocean also coincided with a major magmatic event on the Canadian Arctic margin, Svalbard, Franz Josef Land, and the southern East Siberian Islands circa 125 Ma (see also Corfu et al., 2013). This volcanic event is believed to predate the time of breakup and sea-floor spreading in the Canada Basin and movement along the Khatanga–Bering transform (Doré et al., 2015). Hauterivian–Barremian rejuvenation of sediment source areas along the Sverdrup rim, at the southern part of the Ellesmere Island, along Novaya Zemlya and the land area north of Svalbard and Franz Josef Land (partly including the Alpha–Mendeleev ridge and the Lomonosov Ridge) resulted in increased sediment flux to the nearby basins (Figure 10) (e.g., Dibner, 1998; Gjelberg and Steel, 2012; Tullius et al., 2014). Although the uplift mechanism probably included both an isostatic, rift-related component and a thermal volcanic component, the resulting topography was transient. In the Sverdrup Basin, the sediment pulse decreased during the Albian and the area was dominated by regional transgression in the Cenomanian (Figure 2) (Embry, 1991). Upper Cretaceous rocks are not preserved on Svalbard, but on Franz Josef Land and in the eastern Barents Sea, backstepping and transgression occurred in the latest Albian–Cenomanian (Dibner, 1998; Kayukova and Suslova, 2015). This suggests that the transient topography that formed north of Svalbard and around the Sverdrup Basin lasted for approximately 40 m.y.

Maher et al. (2004) also noted that the regressive Valanginian–Hauterivian clastic wedge on Svalbard is characterized by an upward increase in feldspar and lithic fragments, suggesting that volcanic material was being eroded in the source area to north. Since Early Cretaceous volcanism is widespread also on Franz Josef Land (Dibner, 1998) and in the eastern Barents Sea (Polteau et al., 2016) it is likely that clastic wedges sourced from these areas show similar petrographic characteristics.

Major regression did not occur in the North Slope area until the Aptian, when a pulse of sediment filled most of the deep foreland accommodation (Figure 12) and started to deliver material to the passive margin of the Canada Basin (Bird and Molenaar, 1992; Houseknecht et al., 2009). The North Slope area also experienced transgression during the Cenomanian, but the event was short-lived and the basin was soon dominated by renewed regression (Figure 2). Petrographic data from outcrops in the North Slope area show that the sands deposited in these wedges are rich in lithic fragments and were sourced from volcanic terranes (Johnsson and Sokol, 2000). Mixing of sands from different provenance areas was probably common where sediments were transported axially along the foreland (Smosna et al., 1999), but as foreland accommodation was filled and transport directions were more dip-oriented, it is expected that the margin would show more along-strike variability in provenance and petrographic characteristics.

The same phase of regression also took place to the west in the Hanna trough and North Chukchi Basin (Figures 8, 13) (Houseknecht and Bird, 2011), and Miller et al. (2008) suggested that a foreland basin extended outboard of the SASZ and the Chukotkan fold belt in the Early Cretaceous. Seismic reflection data from the East Siberian shelf also show foreland basin geometry above a Lower Cretaceous unconformity, which is inferred to have formed during the closure of the South Anyui ocean. Initially, this foreland basin would have transported sediments axially toward the North Chukchi Basin, but as the sediment flux increased during peak deformation of the Chukotka fold belt, foreland accommodation was filled and sediments probably bypassed the East Siberian shelf and were delivered to the outer margin of the Canada Basin. Figure 13 shows a significant sedimentary succession above the Lower Cretaceous shelf–slope wedge, which is interpreted to have formed as the result of high sediment input and overfilled basin conditions.

Late Cretaceous and Paleogene Asymmetry

Early Late Cretaceous transgression in the eastern Barents Sea and Franz Josef Land was probably caused by waning of the Early Cretaceous sediment pulse from the north. A similar mechanism may also have controlled basin evolution in the West Siberia and Yenisey–Khatanga Basins, which also experienced transgression at the time (Figure 2). Initial rifting along the Alpha–Mendeleev ridge and in the Laptev area may have captured sediments from the Verkhoyansk fold belt, causing a major decrease in sediment supply to the west (Figure 15). The implication of this model is that backstepping in Yenisey–Khatanga should coincide with the main period of sediment input to the Laptev rift. High axial sediment delivery to the landward tip of the Laptev rift would have resulted in major progradation, and seismic facies from the Upper Cretaceous succession in the Laptev Sea also suggest a predominance of continental deposits. Initially, the axial feeder system delivered sediment to the distal shelf, slope and deep-water parts of what is the present-day Makarov–Podvodnikov Basin (Figures 1, 15). But as rifting of the Eurasia Basin commenced in the early Paleogene and the Lomonosov Ridge was separated from northern Barents Margin, movement along the Khatanga–Bering transform shifted the axial Verkhoyansk feeder system into the newly formed basin (Figure 17). Deep-water segments of the ancient Verkhoyansk feeder system may therefore be present in the outermost part of East Siberian shelf (Figure 2), detached from the primary source area. Later sediment input to this area would have been derived from the inboard topography in the Chukotka fold belt.

Late Cretaceous and Paleogene regression also continued between the North Chukchi Basin and the Mackenzie Delta, with high sediment supply from the nearby Brooks Range, causing progradation into the deep-water Canada Basin (Figure 2). Similarly, uplift associated with the Eurekan orogeny caused sediment delivery to the northern part of the Baffin Bay. The recurring pattern is that the terminal landward sections of these rift basins attracted large sediment feeder systems that were sourced axially into the basins. This included the Laptev, the North Chukchi Basin (Figure 13), the Mackenzie Delta (Figure 18), and the Baffin Bay examples (Figure 17). Sediment input from such axial feeder systems are prone to changes in catchment configuration through time and are generally sensitive to changes in uplift and subsidence onshore.

SUMMARY AND CONCLUSIONS

The Triassic was characterized by deep-water conditions along the paleo-Pacific margin, which was sourced by large fluvial systems from Laurentia and the central Asian fold belt. A central Arctic intracratonic basin connected the greater Barents Sea and the Sverdrup Basin area, receiving sediments from peripheral highlands in Laurentia, Baltica, and the Polar Urals. A sediment-routing system in the West Siberia Basin area is inferred to have supplied sediments to the eastern parts of the Barents Sea prior to uplift of Novaya Zemlya in the Late Triassic–Early Jurassic. The central Arctic landmass (ACMC) was probably characterized by significant topography, generating sediment that were delivered to the Sverdrup, East Siberian shelf, Wrangel Island, and Hanna trough areas.

Regional transgression started in the Early to Middle Jurassic, reaching maximum transgression in the Late Jurassic. Most basins were probably in communication during this period, forming a large Arctic Ocean. The transgression was associated with a decrease in catchment size and a transition to local sediment feeder systems sourced from local topographic highs, especially in the Barents Sea. Rifting in the Canada Basin formed rift–flank topography acting as local provenance areas for the surrounding basins. Accreting terranes along the Pacific margin also resulted in the formation of new sediment source areas toward the end of the period, feeding sediments into the North Slope region. Initial subduction and arrival of the Kolyma–Omolon terrane caused gradual closure of the South Anyui ocean.

A major drainage reorganization occurred in the Early Cretaceous when subduction along the Pacific margin and possibly back-arc extension within the Canada Basin resulted in widespread topographic uplift across the Arctic. The associated sediment pulse was long-lived along the Pacific margin as subduction continued accreting more material to the continent during the Cretaceous and early Cenozoic. But along the Barents Sea margin, uplift was short-lived and transient, and with smaller volumes of sediment being supplied to the basins in the south. Final closure of the South Anyui ocean may have redirected a large sediment routing system from the Lena–Anabar area into the Yenisey–Khatanga Basin.

The Late Cretaceous–Paleogene was dominated by asymmetry across the Arctic with continued regression along the margin of the Canada Basin, but transgression in the Barents Sea and West Siberia Basin. The Eurekan orogeny formed new sediment source areas rerouting of sediments into nearby basins. Opening of the Eurasia Basin may also have rerouted sediments sourced from the Verkhoyansk fold belt, causing a major shift in depocenter from the Makarov–Podvodnikov Basin to the Eurasia Basin. Axial sediment delivery to the tip of the Laptev, Baffin Bay, and Mackenzie Delta rift basins formed the primary depocenters during this time.

Stratigraphic evolution in general and prospectivity assessment in particular reflect the interaction between onshore and offshore sedimentary and environmental processes. Integrated analysis of plate-tectonic evolution and paleogeography serves as a predictive framework for the poorly understood areas of the Arctic.

REFERENCES CITED

Akhmetiev, M. A., N. I. Zaporozhets, V. N. Benyamovskiy, G. N. Aleksandrova, A. I. Iakovleva, and T. V. Oreshkina, 2012, The Paleogene history of the western Siberian seaway—A connection of the Peri–Tethys to the Arctic Ocean: Austrian Journal of Earth Sciences, v. 105, p. 50–67.

Alvey, A., C. Gaina, N. J. Kusznir, and T. H. Torsvik, 2008, Integrated crustal thickness mapping and plate reconstructions for the high Arctic: Earth and Planetary Science Letters, v. 274, no. 3–4, p. 310–321, doi:10.1016/j.epsl.2008.07.036.

Amato, J. M., J. Toro, V. V. Akinin, B. A. Hampton, A. S. Salnikov, and M. I. Tuchkova, 2015, Tectonic evolution of the Mesozoic south Anyui suture zone, eastern Russia: A critical component of paleogeographic reconstructions of the Arctic region: Geosphere, v. 11, no. 5, p. 1530–1564, doi:10.1130/GES01165.1.

Anfinson, O. A., A. F. Embry, and D. F. Stockli, 2016, Geochronologic constraints on the Permian–Triassic northern source region of the Sverdrup Basin, Canadian Arctic Islands: Tectonophysics, v. 691, p. 206–219, doi:10.1016/j.tecto.2016.02.041.

Anfinson, O. A., A. L. Leier, R. Gaschnig, A. F. Embry, and K. Dewing, 2012, U–Pb and Hf isotopic data from Franklinian Basin strata: Insights into the nature of Crockerland and the timing of accretion, Canadian Arctic Islands: Canadian Journal of Earth Sciences, v. 49, no. 11, p. 1316–1328, doi:10.1139/e2012-067.

Berglar, K., D. Franke, R. Lutz, B. Schreckenberger, and V. Damm, 2016, Initial opening of the Eurasian Basin, Arctic Ocean: Frontiers of Earth Science, v. 4, p. 1–14, doi:10.3389/feart.2016.00091.

Bird, K. J., R. R. Charpentier, D. L. Gautier, D. W. Houseknecht, T. R. Klett, J. K. Pitman, T. E. Moore, C. J. Schenk, M. E. Tennyson, and C. J. Wandrey, 2008, Circum–Arctic resource appraisal: Estimates of undiscovered oil and gas north of the Arctic Circle: Denver, Colorado, US Geological Survey Fact Sheet 2008–3049, 4 p.

Bird, K. J., and C. M. Molenaar, 1992, The North Slope foreland basin, Alaska, *in* R. W. Macqueen and D. A. Leckie, eds., Foreland basins and fold belts: AAPG Memoir 55, p. 363–393.

Bondarenko, G., A. Soloviev, M. Tuchkova, J. Garver, and I. Podgornyi, 2003, Age of detrital zircons from sandstones of the Mesozoic flysch formation in the south Anyui suture zone (western Chukotka): Lithology and Mineral Resources, v. 38, no. 2, p. 162–176, doi:10.1023/A:1023456126348.

Bruvoll, V., Y. Kristoffersen, B. J. Coakley, J. R. Hopper, S. Planke, and A. Kandilarov, 2012, The nature of the acoustic basement on Mendeleev and northwestern Alpha ridges, Arctic Ocean: Tectonophysics, v. 514–517, p. 123–145, doi:10.1016/j.tecto.2011.10.015.

Bue, E. P., and A. Andresen, 2014, Constraining depositional models in the Barents Sea region using detrital zircon U–Pb data from Mesozoic sediments in Svalbard, *in* R. A. Scott, H. R. Smyth, A. C. Morton, and N. Richardson, eds., Sediment provenance studies in hydrocarbon exploration and production: Geological Society, London, Special Publications 2014, v. 386, p. 261–279, doi:10.1144/SP386.14.

Buslov, M. M., I. Y. Safonova, G. S. Fedoseev, M. K. Reichow, K. Davies, and G. A. Babin, 2010, Permo–Triassic plume magmatism of the Kuznetsk Basin, central Asia: Geology, geochronology, and geochemistry: Russian Geology and Geophysics, v. 51, no. 9, p. 1021–1036, doi:10.1016/j.rgg.2010.08.010.

Corfu, F., S. Polteau, S. Planke, J. I. Faleide, H. Svensen, A. Zayoncheck, and N. Stolbov, 2013, U–Pb geochronology of Cretaceous magmatism on Svalbard and Franz Josef Land, Barents Sea large igneous province: Geological Magazine, v. 150, no. 6, p. 1127–1135, doi:10.1017/S0016756813000162.

Daragan-Sushchova, L. A., O. V. Petrov, Y. I. Daragan-Sushchov, and M. A. Vasil'ev, 2014, Structure of the North Kara shelf from results of seismostratigraphic analysis: Geotectonics, v. 48, no. 2, p. 139–150, doi:10.1134/S0016852114020022.

Davies, C., M. B. Allen, M. M. Buslov, and I. Safonova, 2010, Deposition in the Kuznetsk Basin, Siberia: Insights into the Permian–Triassic transition and the Mesozoic evolution of central Asia: Palaeogeography, Palaeoclimatology, Palaeoecology, v. 295, no. 1–2, p. 307–322, doi:10.1016/j.palaeo.2010.06.008.

De Paor, D. G., D. C. Bradley, G. Eisenstadt, and S. M. Phillips, 1989, The Arctic Eurekan orogen: A most unusual fold-and-thrust belt: Geological Society of America Bulletin, v. 101, no. 7, p. 952–967, doi:10.1130/0016-7606(1989)101<0952:TAEOAM>2.3.CO;2.

Dewing, K., and A. F. Embry, 2007, Geological and geochemical data from the Canadian Arctic Islands. Part I: Stratigraphic tops from Arctic Islands' oil and gas exploration boreholes: Ottawa, Ontario, Canada, Geological Survey of Canada Open File 5442, 7 p.

Dibner, V. D., ed., 1998, Geology of Franz Josef Land: Oslo, Norway, Norsk Polarinstitutt, Meddelelse no. 146, p. 10–17.

Dixon, J., 1982, Jurassic and Lower Cretaceous subsurface stratigraphy of the Mackenzie Delta–Tuktoyaktuk Peninsula, N.W.T.: Ottawa, Ontario, Canada, Geological Survey of Canada Bulletin 349, 52 p., doi:10.4095/111345.

Dixon, J., 1996, Geological atlas of the Beaufort–Mackenzie area: Ottawa, Ontario, Canada, Geological Survey of Canada Miscellaneous Report 59, 173 p.

Dixon, J., and J. Dietrich, 1990, Canadian Beaufort Sea and adjacent land areas, *in* A. Grantz, L. Johnson, and J. F. Sweeney, eds., The Arctic Ocean region: The geology of North America: Boulder, Colorado, The Geological Society of America, v. L, p. 239–256, doi:10.1130/DNAG-GNA-L.239.

Dixon, J., J. Dietrich, L. Lane, and D. McNeil, 2008, Geology of the Late Cretaceous to Cenozoic Beaufort–Mackenzie basin, *in* A. D. Miall, ed., Sedimentary basins of the world: The sedimentary basins of the United States and Canada: Amsterdam, Elsevier B.V., v. 5, p. 551–572, doi:10.1016/S1874-5997(08)00016-6.

Doré, A. G., E. R. Lundin, A. Gibbons, T. O. Sømme, and B. O. Tørudbakken, 2015, Transform margins of the Arctic: A synthesis and re-evaluation, *in* M. Nemcok, S. Rybár, S. T. Sinha, S. A. Hermeston, and L. Ledvényiová, eds., Transform margins: Development, controls and petroleum system: Geological Society, London, Special Publications 2015, v. 431, p. 63–94, doi:10.1144/sp431.8.

Dörr, N., F. Lisker, P. Clift, A. Carter, D. G. Gee, A. Tebenkov, and C. Spiegel, 2012, Late Mesozoic–Cenozoic exhumation history of northern Svalbard and its regional significance: Constraints from apatite fission track analysis: Tectonophysics, v. 514, p. 81–92, doi:10.1016/j.tecto.2011.10.007.

Døssing, A., H. R. Jackson, J. Matzka, I. Einarsson, T. M. Rasmussen, A. V. Olesen, and J. M. Brozena, 2013, On the origin of the Amerasia Basin and the high Arctic large igneous province—Results of new aeromagnetic data: Earth and Planetary Science Letters, v. 363, p. 219–230, doi:10.1016/j.epsl.2012.12.013.

Drachev, S. S., 2011, Tectonic setting, structure and petroleum geology of the Siberian Arctic offshore sedimentary basins, *in* A. M. Spencer, A. F. Embry, D. L. Gautier, A. V. Stoupakova, and K. Sørensen, eds., Arctic petroleum geology: Geological Society, London, Memoirs 2011, v. 35, p. 369–394, doi:10.1144/M35.25.

Drachev, S. S., N. Kaul, and V. N. Beliaev, 2003, Eurasia spreading basin to Laptev Shelf transition: Structural pattern and heat flow: Geophysical Journal International, v. 152, no. 3, p. 688–698, doi:10.1046/j.1365-246X.2003.01882.x.

Drachev, S. S., N. A. Malyshev, and A. M. Nikishin, 2010, Tectonic history and petroleum geology of the Russian Arctic shelves: An overview, *in* B. A. Vining and S. C. Pickering, eds., Petroleum Geology: From Mature Basins to New Frontiers—Proceedings of the 7th Petroleum Geology Conference, London, March 30–April 2, 2009, p. 591–619, doi:10.1144/0070591.

Drachev, S. S., L. A. Savostin, V. G. Groshev, and I. E. Bruni, 1998, Structure and geology of the continental shelf of the Laptev Sea, eastern Russian Arctic: Tectonophysics, v. 298, no. 4, p. 357–393, doi:10.1016/S0040-1951(98)00159-0.

Dutro, J. T. Jr., 1981, Geology of Alaska bordering the Arctic Ocean, *in* A. M. Nairn, M. Churkin Jr., and F. G. Stehli, eds., The ocean basins and margins: The Arctic Ocean: New York, Springer, v. 5, p. 21–36, doi:10.1007/978-1-4757-1248-3_2.

Dypvik, H., E. Håkansson, and C. Heinberg, 2002, Jurassic and Cretaceous palaeogeography and stratigraphic comparisons in the North Greenland–Svalbard region: Polar Research, v. 21, no. 1, p. 91–108, doi:10.3402/polar.v21i1.6476.

Dypvik, H., A. Sokolov, T. Pcelina, B. Fjellså, T. Bjærke, M. Korchinskaja, and J. Nagy, 1998, The Triassic successions of Franz Josef Land, stratigraphy and sedimentology of three wells from Alexandra, Hayes and Graham–Bell islands, *in* A. Solheim, E. Musatov, and N. Heintz, eds., Geological aspects of Franz Josef Land

and the northernmost Barents Sea—The northern Barents Sea geotraverse: Oslo, Norway, Norsk Polarinstitutt, Meddelelser no. 151, p. 50–82.

Egorov, A. Y., and A. Mørk, 2000, The east Siberian and Svalbard Triassic successions and their sequence stratigraphical relationships: Zentralblatt für Geologie und Paläontologie, Teil I, v. 1, p. 1377–1430.

Eide, C. H., T. G. Klausen, D. Katkov, A. A. Suslova, and W. Helland-Hansen, 2018, Linking an early Triassic delta to antecedent topography: Source-to-sink study of the southwestern Barents Sea margin: GSA Bulletin, v. 130, no. 1–2, p. 263–283, doi:10.1130/B31639.1.

Embry, A., 2009, Crockerland—The source area for the Triassic to Middle Jurassic strata of northern Axel Heiberg Island, Canadian Arctic Islands: Bulletin of Canadian Petroleum Geology, v. 57, no. 2, p. 129–140, doi: 10.2113/gscpgbull.57.2.129.

Embry, A. F., 1991, Mesozoic history of the Arctic Islands, *in* H. P. Trettin, ed., Geology of the Innuitian orogen and Arctic platform of Canada and Greenland: Ottawa, Ontario, Canada, Geological Survey of Canada Geology of Canada Series 3, p. 370–433, doi:10.4095/133959.

Embry, A. F., 1993a, Crockerland—The northwest source area for the Sverdrup Basin, Canadian Arctic Islands, *in* T. O. Vorren, E. Bergsager, Ø. A. Dahl-Stamnes, E. Holter, B. Johansen, E. Lie, and T. B. Lund, eds., Arctic geology and petroleum potential: Norwegian Petroleum Society Special Publication 2, p. 205–216, doi:10.1016/b978-0-444-88943-0.50018-6.

Embry, A. F., 1993b, Transgressive–regressive (T–R) sequence analysis of the Jurassic succession of the Sverdrup Basin, Canadian Arctic archipelago: Canadian Journal of Earth Sciences, v. 30, no. 2, p. 301–320, doi:10.1139/e93-024.

Embry, A. F., and B. Beauchamp, 2008, Sverdrup basin, *in* A. D. Miall, ed., Sedimentary basins of the world: The sedimentary basins of the United States and Canada: Amsterdam, Elsevier B.V., v. 5, p. 451–471, doi: 10.1016/S1874-5997(08)00013-0.

Embry, A. F., and J. Dixon, 1994, The age of the Amerasia Basin, *in* D. K. Thurston and K. Fujita, eds., International Conference on Arctic Margins, Magadan, Russia, September 6–10, 1994, , p. 289–295.

Ershova, V. B., J. M. Holbrook, A. K. Khudoley, and A. V. Prokopiev, 2010, Sequence stratigraphy of the Lower Cretaceous deposits of the Chekurovka area (NE Siberia, Lena R.)—Preliminary results: 4th EAGE St. Petersburg International Conference and Exhibition on Geosciences—New Discoveries through Integration of Geosciences, St. Petersburg, Russia, April 5–10, 2010, doi:10.3997/2214-4609.20145413.

Ershova, V. B., A. K. Khudoley, A. V. Prokopiev, M. I. Tuchkova, P. V. Fedorov, G. G. Kazakova, S. B. Shishlov, and P. O'Sullivan, 2016, Trans-Siberian Permian rivers: A key to understanding Arctic sedimentary provenance: Tectonophysics, v. 691, p. 220–233, doi:10.1016/j.tecto.2016.03.028.

Evangelatos, J., and D. C. Mosher, 2016, Seismic stratigraphy, structure and morphology of Makarov Basin and surrounding regions: Tectonic implications: Marine Geology, v. 374, p. 1–13, doi:10.1016/j.margeo.2016.01.013.

Faleide, J. I., F. Tsikalas, A. J. Breivik, R. Mjelde, O. Ritzmann, O. Engen, J. Wilson, and O. Eldholm, 2008, Structure and evolution of the continental margin off Norway and the Barents Sea: Episodes, v. 31, p. 82–91.

Faleide, J. I., E. Vågnes, and S. T. Gudlaugsson, 1993, Late Mesozoic–Cenozoic evolution of the southwestern Barents Sea, *in* J. R. Parker, ed., Petroleum Geology of Northwest Europe: Proceedings of the 4th Conference, London, March 29–April 1, 1992, p. 933–950.

Fleming, E. J., M. J. Flowerdew, H. R. Smyth, R. A. Scott, A. C. Morton, J. E. Omma, D. Frei, and M. J. Whitehouse, 2016, Provenance of Triassic sandstones on the southwest Barents Shelf and the implication for sediment dispersal patterns in northwest Pangaea: Marine and Petroleum Geology, v. 78, p. 516–535, doi:10.1016/j.marpetgeo.2016.10.005.

Franke, D., K. Hinz, and O. Oncken, 2001, The Laptev sea rift: Marine and Petroleum Geology, v. 18, no. 10, p. 1083–1127, doi:10.1016/S0264-8172(01)00041-1.

Gjelberg, J., and R. Steel, 2012, Depositional model for the Lower Cretaceous Helvetiafjellet Formation on Svalbard—Diachronous versus layer-cake models: Norsk Geologisk Tidsskrift, v. 92, p. 41–54.

Gjelberg, J., and R. J. Steel, 1995, Helvetiafjellet Formation (Barremian–Aptian), Spitsbergen: Characteristics of a transgressive succession, *in* R. J. Steel, V. L. Felt, E. P. Johannessen, and C. Mathieu, eds., Sequence stratigraphy on the northwest European margin: Proceedings of the Norwegian Petroleum Society Conference, Stavanger, Norway, February 1–3, 1993, p. 571–593, doi: 10.1016/S0928-8937(06)80087-1.

Glorie, S., and J. De Grave, 2016, Exhuming the Meso–Cenozoic Kyrgyz Tianshan and Siberian Altai–Sayan: A review based on low-temperature thermochronology: Geoscience Frontiers, v. 7, no. 2, p. 155–170, doi: 10.1016/j.gsf.2015.04.003.

Glørstad-Clark, E., J. I. Faleide, B. A. Lundschien, and J. P. Nystuen, 2010, Triassic seismic sequence stratigraphy and paleogeography of the western Barents Sea area: Marine and Petroleum Geology, v. 27, no. 7, p. 1448–1475, doi:10.1016/j.marpetgeo.2010.02.008.

Golonka, J., 2011, Phanerozoic palaeoenvironment and palaeolithofacies maps of the Arctic region, *in* A. M. Spencer, A. F. Embry, D. L. Gautier, A. V. Stoupakova, and K. Sørensen, eds., Arctic petroleum geology: Geological Society, London, Memoirs 2011, v. 35, p. 79–129, doi: 10.1144/M35.6.

Golonka, J., N. Y. Bocharova, D. Ford, M. E. Edrich, J. Bednarczyk, and J. Wildharber, 2003, Paleogeographic reconstructions and basins development of the Arctic: Marine and Petroleum Geology, v. 20, no. 3-4, p. 211–248, doi:10.1016/S0264-8172(03)00043-6.

Gottlieb, E. S., K. E. Meisling, E. L. Miller, and G. Charles, 2014, Closing the Canada Basin: Detrital zircon geochronology relationships between the north slope of Arctic Alaska and the Franklinian mobile belt of Arctic

Canada: Geosphere, v. 10, no. 6, p. 1366–1384, doi: 10.1130/GES01027.1.
Gramberg, I. S., 1988, Barents shelf platform: Leningrad, Russia, Nedra, PGO "Sevmorgeologiya," 263 p.
Grantz, A., S. Eittreim, and D. A. Dinter, 1979, Geology and tectonic development of the continental-margin north of Alaska: Tectonophysics, v. 59, no. 1–4, p. 263–291, doi: 10.1016/0040-1951(79)90050-7.
Grantz, A., P. E. Hart, and V. A. Childers, 2011, Geology and tectonic development of the Amerasia and Canada Basins, Arctic Ocean, *in* A. M. Spencer, A. F. Embry, D. L. Gautier, A. V. Stoupakova, and K. Sørensen, eds., Arctic petroleum geology: Geological Society, London, Memoirs 2011, v. 35, p. 771–799, doi:10.1144/M35.50.
Gregersen, U., J. R. Hopper, and P. C. Knutz, 2013, Basin seismic stratigraphy and aspects of prospectivity in the NE Baffin Bay, northwest Greenland: Marine and Petroleum Geology, v. 46, p. 1–18, doi:10.1016/j.marpetgeo.2013.05.013.
Grist, A. M., and M. Zentilli, 2006, Preliminary apatite fission track thermal history modelling of the Nares region of eastern Ellesmere Island and northwestern Greenland: Polarforschung, v. 74, p. 113–127.
Gustavsen, F. B., H. Dypvik, and A. Solheim, 1997, Shallow geology of the northern Barents Sea: Implications for petroleum potential: AAPG Bulletin, v. 81, no. 11, p. 1827–1842.
Hadlari, T., D. Midwinter, J. M. Galloway, K. Dewing, and A. M. Durbano, 2016, Mesozoic rift to post-rift tectonostratigraphy of the Sverdrup Basin, Canadian Arctic: Marine and Petroleum Geology, v. 76, p. 148–158, doi: 10.1016/j.marpetgeo.2016.05.008.
Hamilton, W. B., 2007, Driving mechanism and 3-D circulation of plate tectonics, *in* J. W. Sears, T. A. Harms, and C. A. Evenchick, eds., Whence the mountains? Inquiries into the evolution of Orogenic systems: A volume in honor of Raymond A. Price: Boulder, Colorado, Geological Society of America Special Paper 433, p. 1–25, doi:10.1130/2007.2433(01).
Harris, D., J. Toro, and A. Prokopiev, 2013, Detrital zircon U-Pb geochronology of Mesozoic sandstones from the lower Yana River, northern Russia: Lithosphere, v. 5, no. 1, p. 98–108, doi:10.1130/L250.1.
Harrison, J. C., and T. A. Brent, 2005, Basins and fold belts of Prince Patrick Island and adjacent areas, Canadian Arctic Islands: Ottawa, Ontario, Canada, Geological Survey of Canada Bulletin 560, 208 p.
Harrison, J. C., T. A. Brent, and G. N. Oakey, 2011, Baffin Fan and its inverted rift system of Arctic eastern Canada: stratigraphy, tectonics and petroleum resource potential, *in* A. M. Spencer, A. F. Embry, D. L. Gautier, A. V. Stoupakova, and K. Sørensen, eds., Arctic petroleum geology: Geological Society, London, Memoirs 2011, v. 35, p. 595–626, doi:10.1144/M35.40.
Helwig, J., N. Kumar, P. Emmet, and M. Dinkelman, 2011, Regional seismic interpretation of crustal framework, Canadian Arctic passive margin, Beaufort Sea, with comments on petroleum potential, *in* A. M. Spencer, A. F. Embry, D. L. Gautier, A. V. Stoupakova, and K. Sørensen, eds., Arctic petroleum geology: Geological Society, London, Memoirs 2011, v. 35, p. 527–543, doi: 10.1144/M35.35.
Henriksen, E., A. E. Ryseth, G. B. Larssen, T. Heide, K. Rønning, K. Sollid, and A. V. Stoupakova, 2011, Tectonostratigraphy of the greater Barents Sea: Implications for petroleum systems, *in* A. M. Spencer, A. F. Embry, D. L. Gautier, A. V. Stoupakova, and K. Sørensen, eds., Arctic petroleum geology: Geological Society, London, Memoirs 2011, v. 35, p. 163–195, doi: 10.1144/M35.10.
Herron, E. M., J. F. Dewey, and W.-C. I. Pitman, 1974, Plate tectonic model for the evolution of the Arctic: Geology, v. 2, no. 8, p. 377–380, doi:10.1130/0091-7613(1974)2<377:PTMFTE>2.0.CO;2.
Houseknecht, D. W., and K. J. Bird, 2011, Geology and petroleum potential of the rifted margins of the Canada Basin, *in* A. M. Spencer, A. F. Embry, D. L. Gautier, A. V. Stoupakova, and K. Sørensen, eds., Arctic petroleum geology: Geological Society, London, Memoirs 2011, v. 35, p. 509–526, doi:10.1144/M35.34.
Houseknecht, D. W., K. J. Bird, and C. J. Schenk, 2009, Seismic analysis of clinoform depositional sequences and shelf-margin trajectories in Lower Cretaceous (Albian) strata, Alaska north slope: Basin Research, v. 21, no. 5, p. 644–654, doi:10.1111/j.1365-2117.2008.00392.x.
Høy, T., and B. A. Lundschien, 2011, Triassic deltaic sequences in the northern Barents Sea, *in* A. M. Spencer, A. F. Embry, D. L. Gautier, A. V. Stoupakova, and K. Sørensen eds., Arctic petroleum geology: Geological Society, London, Memoirs 2011, v. 35, p. 249–260, doi: 10.1144/m35.15.
Håkansson, E., and S. A. S. Pedersen, 2001, The Wandel Hav strike-slip mobile belt—A Mesozoic plate boundary in North Greenland: Bulletin of the Geological Society of Denmark, v. 48, p. 149–158.
Inger, S., R. A. Scott, and B. G. Golionko, 1999, Tectonic evolution of the Taimyr peninsula, northern Russia: Implications for Arctic continental assembly: Journal of the Geological Society, v. 156, no. 6, p. 1069–1072, doi: 10.1144/gsjgs.156.6.1069.
Johnsson, M. J., 1993, The system controlling the composition of clastic sediments, in M. J. Johnsson and A. Basu, eds., Processes controlling the composition of clastic sediments: Boulder, Colorado, Geological Society of America Special Paper 284, p. 1–19, doi:10.1130/SPE284-p1.
Johnsson, M. J., and N. K. Sokol, 2000, Stratigraphic variation in petrographic composition of Nanushuk Group sandstones at Slope Mountain, North Slope, Alaska, *in* K. D. Kelley and L. P. Gough, eds., Geologic studies in Alaska by the US Geological Survey, 1998: Denver, Colorado, US Geological Survey Professional Paper 1615, p. 83–100.
Kaminsky, V., O. Suprunenko, and V. Suslova, 2011, Oil and gas potential of the Russian Arctic shelf and palaeogeographical mapping of the Barents Sea, *in* A. M. Spencer, A. F. Embry, D. L. Gautier, A. V. Stoupakova, and K. Sørensen, eds., Arctic petroleum geology: Geological

Society, London, Memoirs 2011, v. 35, p. 345–352, doi:10.1144/M35.22.
Kayukova, A., and A. Suslova, 2015, A seismostratigraphic analysis of the lower cretaceous deposits of the Barents sea to reveal petroleum perspectives: Moscow University Geology Bulletin, v. 70, no. 2, p. 177–182, doi:10.3103/S0145875215020040.
Khudoley, A., and G. Guriev, 1994, The formation and development of a late Paleozoic sedimentary basin on the passive margin of the Siberian paleocontinent, *in* A. F. Embry, B. Beauchamp, and D. J. Glass, eds., Pangea: Global environments and resources: Calgary, Alberta, Canada, Canadian Society of Petroleum Geologists Memoir 17, p. 131–143.
Khudoley, A. K., and A. V. Prokopiev, 2007, Defining the eastern boundary of the North Asian craton from structural and subsidence history studies of the Verkhoyansk fold-and-thrust belt, *in* J. W. Sears, T. A. Harms, and C. A. Evenchick, eds., Whence the mountains? Inquiries into the evolution of Orogenic systems: A volume in honor of Raymond A. Price: Boulder, Colorado, Geological Society of America Special Paper 433, p. 391–410, doi:10.1130/2007.2433(19).
Klausen, T. G., and A. Mørk, 2014, The Upper Triassic paralic deposits of the De Geerdalen Formation on Hopen: Outcrop analog to the subsurface Snadd Formation in the Barents Sea: AAPG Bulletin, v. 98, no. 10, p. 1911–1941, doi:10.1306/02191413064.
Klausen, T. G., R. Müller, J. Slama, and W. Helland-Hansen, 2017, Evidence for Late Triassic provenance areas and Early Jurassic sediment supply turnover in the Barents Sea Basin of northern Pangea: Lithosphere, v. 9, no. 1, p. 14–28, doi:10.1130/L556.1.
Knutz, P. C., U. G. Gregersen, and J. R. Hopper, 2012, Late Paleogene submarine fans in Baffin Bay and northwest Greenland: 74th EAGE Conference & Exhibition Incorporating SPE EUROPEC 2012, Copenhagen, Denmark, June 4, 2012, 4 p., doi:10.3997/2214-4609.20148203.
Konstantinovsky, A. A., and L. N. Lipchanskaya, 2011, Structure and sedimentary formations of the northern Yana–Kolyma Fold System, Yakutia: Geotectonics, v. 45, no. 6, p. 453–468, doi:10.1134/S0016852111060033.
Kontorovich, A., S. Ershov, V. Kazanenkov, Y. N. Karogodin, V. Kontorovich, N. Lebedeva, B. Nikitenko, N. Popova, and B. Shurygin, 2014, Cretaceous paleogeography of the west Siberian sedimentary basin: Russian Geology and Geophysics, v. 55, no. 5–6, p. 582–609, doi:10.1016/j.rgg.2014.05.005.
Kontorovich, A., V. Kontorovich, S. Ryzhkova, B. Shurygin, L. Vakulenko, E. Gaideburova, V. Danilova, V. Kazanenkov, N. Kim, and E. Kostyreva, 2013, Jurassic paleogeography of the west Siberian sedimentary basin: Russian Geology and Geophysics, v. 54, no. 8, p. 747–779, doi:10.1016/j.rgg.2013.07.002.
Kos'ko, M., and E. Korago, 2009, Review of geology of the new Siberian islands between the Laptev and the east Siberian seas, north east Russia, *in* D. B. Stone, K. Fujita, P. W. Layer, E. L. Miller, A. V. Prokopiev, and J. Toro, eds., Geology, geophysics and tectonics of Northeastern Russia: A tribute to Leonid Parfenov: Stephan Mueller Special Publication Series 4, p. 45–64.
Kos'ko, M., and G. Trufanov, 2002, Middle Cretaceous to Eopleistocene sequences on the new Siberian Islands: an approach to interpret offshore seismic: Marine and Petroleum Geology, v. 19, no. 7, p. 901–919, doi:10.1016/S0264-8172(02)00057-0.
Kuzmichev, A. B., 2009, Where does the south Anyui suture go in the new Siberian islands and Laptev Sea?: Implications for the Amerasia basin origin: Tectonophysics, v. 463, no. 1–4, p. 86–108, doi:10.1016/j.tecto.2008.09.017.
Kyzs'michev, A. B., A. V. Soloviev, V. E. Gonikberg, M. N. Shapiro, and O. V. Zamzhitskii, 2006, Mesozoic syncollision siliciclastic sediments of the Bols'shoi Lyakhov Island (New Siberian Islands): Stratigraphy and Geological Correlation, v. 14, no. 1, p. 30–48, doi:10.1134/S0869593806010035.
Lawver, L. A., L. M. Gahagan, and I. Norton, 2011, Palaeogeographic and tectonic evolution of the Arctic region during the Palaeozoic, *in* A. M. Spencer, A. F. Embry, D. L. Gautier, A. V. Stoupakova, and K. Sørensen, eds., Arctic petroleum geology: Geological Society, London, Memoirs 2011, v. 35, p. 61–77, doi:10.1144/M35.5.
Le Heron, D. P., M. M. Buslov, C. Davies, K. Richards, and I. Safonova, 2008, Evolution of Mesozoic fluvial systems along the SE flank of the west Siberian Basin, Russia: Sedimentary Geology, v. 208, no. 1–2, p. 45–60, doi:10.1016/j.sedgeo.2008.05.001.
Lease, R. O., D. W. Houseknecht, and A. R. Kylander-Clark, 2014, Absolute age constraints on rapid, axial progradation of a high-relief clinoform depositional system in the Colville Foreland Basin, Arctic Alaska, *in* AGU Fall Meeting Abstracts: AGU Fall Meeting, San Francisco, California, December 15–19, 2014, p. 35–49.
Lebedeva-Ivanova, N. N., Y. Y. Zamansky, A. E. Langinen, and M. Y. Sorokin, 2006, Seismic profiling across the Mendeleev Ridge at 82°N: Evidence of continental crust: Geophysical Journal International, v. 165, no. 2, p. 527–544, doi:10.1111/j.1365-246X.2006.02859.x.
Ledneva, G. V., V. L. Pease, and S. D. Sokolov, 2011, Permo-Triassic hypabyssal mafic intrusions and associated tholeiitic basalts of the Kolyuchinskaya Bay, Chukotka (NE Russia): Links to the Siberian LIP: Journal of Asian Earth Sciences, v. 40, no. 3, p. 737–745, doi:10.1016/j.jseaes.2010.11.007.
Leith, T. L., H. M. Weiss, A. Mørk, N. Århus, G. Elvebakk, A. F. Embry, P. W. Brooks et al., 1993, Mesozoic hydrocarbon source-rocks of the Arctic region, *in* T. O. Vorren, E. Bergsager, Ø. A. Dahl-Stamnes, E. Holter, B. Johansen, E. Lie, and T. B. Lund, eds., Arctic geology and petroleum potential: Oslo, Norway, Norwegian Petroleum Society Special Publication 2, p. 1–25.
Lundin, E., and A. Doré, 2017, The Gulf of Mexico and Canada Basin: Genetic siblings on either side of North America: Geological Society of America Today, v. 27, p. 4–11, doi:10.1130/GSATG274A.1.

Lundschien, B. A., T. Høy, and A. Mørk, 2014, Triassic hydrocarbon potential in the Northern Barents Sea; integrating Svalbard and stratigraphic core data: Norwegian Petroleum Directorate Bulletin, v. 11, p. 3–20.

Maher, J., T. Hays, R. Shuster, and J. Mutrux, 2004, Petrography of Lower Cretaceous sandstones on Spitsbergen: Polar Research, v. 23, no. 2, p. 147–165, doi: 10.3402/polar.v23i2.6276.

Marín, D., A. Escalona, K. K. Śliwińska, H. Nøhr-Hansen, and A. Mordasova, 2017, Sequence stratigraphy and lateral variability of Lower Cretaceous clinoforms in the SW Barents Sea: AAPG Bulletin, v. 101, no. 9, p. 1487–1517, doi:10.1306/10241616010.

Melvin, J., and A. S. Knight, 1984, Lithofacies, diagenesis and porosity of the Ivishak Formation, Prudhoe Bay Area, Alaska: Part 3. Applications in exploration and production, *in* D. A. McDonald and R. C. Surdam, eds., Clastic diagenesis:AAPG Memoir 37, p. 347–365.

Meneley, R., D. Henao, and R. Merritt, 1975, The northwest margin of the Sverdrup Basin, *in* C. J. Yorath, E. R. Parker, and D. J. Glass, eds., Canada's continental margins and offshore petroleum exploration: Calgary, Alberta, Canada, Canadian Society of Petroleum Geologists Memoir 4, p. 531–544.

Mickey, M. B., A. Bymes, and H. Haga, 2002, Biostratigraphic evidence for the prerift position of the North Slope, Alaska, and Arctic Islands, Canada, and Sinemurian incipient rifting of the Canada Basin, *in* E. L. Miller, A. Grantz, and S. Klemperer, eds., Tectonic evolution of the Bering shelf–Chukchi Sea–Arctic margin and adjacent landmasses: Boulder, Colorado, Geological Society of America Special Paper 360, p. 67–76, doi:10.1130-8137-2360-4.67.

Midtkandal, I., and J. Nystuen, 2009, Depositional architecture of a low-gradient ramp shelf in an epicontinental sea: The lower Cretaceous of Svalbard: Basin Research, v. 21, no. 5, p. 655–675, doi:10.1111/j.1365-2117.2009.00399.x.

Midwinter, D., T. Hadlari, W. Davis, K. Dewing, and R. Arnott, 2016, Dual provenance signatures of the Triassic northern Laurentian margin from detrital-zircon U-Pb and Hf-isotope analysis of Triassic–Jurassic strata in the Sverdrup Basin: Lithosphere, v. 8, no. 6, p. 668–683, doi:10.1130/L517.1.

Miller, E., G. Gehrels, V. Pease, and S. Sokolov, 2010, Stratigraphy and U-Pb detrital zircon geochronology of Wrangel Island, Russia: Implications for Arctic paleogeography: AAPG Bulletin, v. 94, no. 5, p. 665–692, doi: 10.1306/10200909036.

Miller, E. L., and V. E. Verzhbitsky, 2009, Structural studies near Pevek, Russia: Implications for formation of the east Siberian shelf and Makarov Basin of the Arctic Ocean, *in* D. B. Stone, K. Fujita, P. W. Layer, E. L. Miller, A. V. Prokopiev, and J. Toro, eds., Geology, geophysics and tectonics of Northeastern Russia: A tribute to Leonid Parfenov: Stephan Mueller Special Publication Series 4, p. 223–241, doi:10.5194/smsps-4-223-2009.

Miller, E. L., A. Soloviev, A. Kuzmichev, G. Gehrels, J. Toro, and M. Tuchkova, 2008, Jurassic and Cretaceous foreland basin deposits of the Russian Arctic: Separated by birth of the Makarov Basin?: Norsk Geologisk Tidsskrift, v. 88, p. 201–226.

Miller, E. L., A. V. Soloviev, A. V. Prokopiev, J. Toro, D. Harris, A. B. Kuzmichev, and G. E. Gehrels, 2013, Triassic river systems and the paleo-Pacific margin of northwestern Pangea: Gondwana Research, v. 23, no. 4, p. 1631–1645, doi:10.1016/j.gr.2012.08.015.

Miller, E. L., J. Toro, G. Gehrels, J. M. Amato, A. Prokopiev, M. I. Tuchkova, V. V. Akinin, T. A. Dumitru, T. E. Moore, and M. P. Cecile, 2006, New insights into Arctic paleogeography and tectonics from U-Pb detrital zircon geochronology: Tectonics, v. 25, no. 3, p. 1–19, doi:10.1029/2005TC001830.

Moore, T. E., T. A. Dumitru, K. E. Adams, S. N. Witebsky, and A. G. Harris, 2002, Origin of the Lisburne Hills-Herald Arch structural belt: Stratigraphic, structural, and fission-track evidence from the Cape Lisburne area, northwestern Alaska, *in* E. L. Miller, A. Grantz, and S. Klemperer, eds., Tectonic evolution of the Bering shelf–Chukchi Sea–Arctic margin and adjacent landmasses: Boulder, Colorado, Geological Society of America Special Paper 360, p. 77–110, doi:10.1130/0-8137-2360-4.77.

Moore, T. E., P. B. O'Sullivan, C. J. Potter, and R. A. Donelick, 2015, Provenance and detrital zircon geochronologic evolution of lower Brookian foreland basin deposits of the western Brooks Range, Alaska, and implications for early Brookian tectonism: Geosphere, v. 11, no. 1, p. 93–122, doi:10.1130/GES01043.1.

Moore, T. E., W. K. Wallace, K. J. Bird, S. M. Karl, C. G. Mull, and J. T. Dillon, 1994, Geology of northern Alaska, *in* G. Plafker and H. C. Berg, eds., The geology of Alaska: Boulder, Colorado, Geological Society of America, The Geology of North America, v. G-1, p. 49–140.

Müller, R., J. P. Nystuen, F. Eide, and H. Lie, 2005, Late Permian to Triassic basin infill history and palaeogeography of the Mid-Norwegian shelf—East Greenland region, *in* B. T. G. Wandås, J. P. Nystuen, E. Eide, and F. Gradstein, eds., Onshore-offshore relationships on the north Atlantic margin: Oslo, Norway, Norwegian Petroleum Society Special Publication 12, p. 165–189, doi:10.1016/S0928-8937(05)80048-7.

Musatov, E., and Y. Pogrebitskij, 2000, Late Mesozoic–Cenozoic evolution of the Barents Sea and Kara Sea continental margins: Polarforschung, v. 68, p. 283–290.

Nikishin, A. M., E. I. Petrov, N. A. Malyshev, and V. P. Ershova, 2017, Rift systems of the Russian eastern arctic shelf and arctic deep water basins: Link between geological history and geodynamics: Geodynamics and Tectonophysics, v. 8, p. 11–43.

Nokleberg, W. J., L. M. Parfenov, J. W. H. Monger, I. O. Norton, A. I. Khanchuk, D. B. Stone, C. R. Scotese, D. W. Scholl, and K. Fujita, 2001, Phanerozoic tectonic evolution of the Circum–North Pacific: Denver, Colorado, US Geological Survey Professional Paper 1626, p. 1–102.

Omma, J., V. Pease, and R. Scott, 2011, U–Pb SIMS zircon geochronology of Triassic and Jurassic sandstones on northwestern Axel Heiberg Island, northern Sverdrup Basin, Arctic Canada, *in* A. M. Spencer, A. F. Embry,

D. L. Gautier, A. V. Stoupakova, and K. Sørensen, eds., Arctic petroleum geology: Geological Society, London, Memoirs 2011, v. 35, p. 559–566, doi:10.1144/M35.37.

Oxman, V. S., 2003, Tectonic evolution of the Mesozoic Verkhoyansk–Kolyma belt (NE Asia): Tectonophysics, v. 365, no. 1–4, p. 45–76, doi:10.1016/S0040-1951(03)00064-7.

Patchett, P., A. Embry, G. Ross, B. Beauchamp, J. Harrison, U. Mayr, C. Isachsen, E. Rosenberg, and G. Spence, 2004, Sedimentary cover of the Canadian Shield through Mesozoic time reflected by Nd isotopic and geochemical results for the Sverdrup Basin, Arctic Canada: Journal of Geology, v. 112, no. 1, p. 39–57, doi:10.1086/379691.

Peters, K., L. Magoon, K. Bird, Z. Valin, and M. Keller, 2006, North Slope, Alaska: Source rock distribution, richness, thermal maturity, and petroleum charge: AAPG Bulletin, v. 90, no. 2, p. 261–292, doi:10.1306/09210505095.

Petersen, T. G., T. B. Thomsen, S. Olaussen, and L. Stemmerik, 2016, Provenance shifts in an evolving Eurekan foreland basin: The Tertiary Central Basin, Spitsbergen: Journal of the Geological Society, v. 173, no. 4, p. 634–648, doi:10.1144/jgs2015-076.

Petrov, O. V., N. N. Sobolev, T. N. Koren, V. E. Vasiliev, E. O. Petrov, G. B. Larssen, and M. Smelror, 2008, Palaeozoic and Early Mesozoic evolution of the east Barents and Kara Seas sedimentary basins: Norsk Geologisk Tidsskrift, v. 88, p. 227–234.

Pinous, O., M. Levchuk, and D. Sahagian, 2001, Regional synthesis of the productive Neocomian complex of west Siberia: Sequence stratigraphic framework: AAPG Bulletin, v. 85, no. 10, p. 1713–1730.

Polteau, S., B. W. Hendriks, S. Planke, M. Ganerød, F. Corfu, J. I. Faleide, I. Midtkandal, H. S. Svensen, and R. Myklebust, 2016, The Early Cretaceous Barents Sea sill complex: Distribution, $^{40}Ar/^{39}Ar$ geochronology, and implications for carbon gas formation: Palaeogeography, Palaeoclimatology, Palaeoecology, v. 441, p. 83–95, doi:10.1016/j.palaeo.2015.07.007.

Portenga, E. W., and P. R. Bierman, 2011, Understanding earth's eroding surface with ^{10}Be: Geological Society of America Today, v. 21, no. 8, p. 4–10, doi:10.1130/G111A.1.

Prokopiev, A. V., J. Toro, E. L. Miller, and G. E. Gehrels, 2008, The paleo-Lena River–200 m.y. of transcontinental zircon transport in Siberia: Geology, v. 36, no. 9, p. 699–702, doi:10.1130/G24924A.1.

Puchkov, V. N., 2013, Structural stages and evolution of the Urals: Mineralogy and Petrology, v. 107, no. 1, p. 3–37, doi:10.1007/s00710-012-0263-1.

Ricketts, B. D., and R. A. Stephenson, 1994, The demise of Sverdrup Basin: Late Cretaceous–Paleogene sequence stratigraphy and forward modeling: Journal of Sedimentary Research, v. 64, doi:10.1306/D4267FF5-2B26-11D7-8648000102C1865D.

Riis, F., B. A. Lundschien, T. Høy, A. Mørk, and M. B. E. Mørk, 2008, Evolution of the Triassic shelf in the northern Barents Sea region: Polar Research, v. 27, no. 3, p. 318–338, doi:10.1111/j.1751-8369.2008.00086.x.

Riis, F., J. Vollset, and M. Sand, 1986, Tectonic development of the western margin of the Barents Sea and adjacent areas, *in* M. T. Halbouty, ed., Future petroleum provinces of the world: AAPG Memoir 40, p. 661–675.

Røhr, T. S., T. Andersen, and H. Dypvik, 2008, Provenance of Lower Cretaceous sediments in the Wandel Sea Basin, north Greenland: Journal of the Geological Society, v. 165, no. 3, p. 755–767, doi:10.1144/0016-76492007-102.

Røhr, T. S., T. Andersen, H. Dypvik, and A. F. Embry, 2010, Detrital zircon characteristics of the Lower Cretaceous Isachsen Formation, Sverdrup Basin: Source constraints from age and Hf isotope data: Canadian Journal of Earth Sciences, v. 47, no. 3, p. 255–271, doi:10.1139/E10-006.

Schröder-Adams, C., 2014, The Cretaceous polar and western interior seas: Paleoenvironmental history and paleoceanographic linkages: Sedimentary Geology, v. 301, p. 26–40, doi:10.1016/j.sedgeo.2013.12.003.

Sekretov, S. B., 2001, Northwestern margin of the east Siberian Sea, Russian Arctic: Seismic stratigraphy, structure of the sedimentary cover and some remarks on the tectonic history: Tectonophysics, v. 339, no. 3–4, p. 353–371, doi:10.1016/S0040-1951(01)00108-1.

Setoyama, E., M. A. Kaminski, and J. Tyszka, 2011, The Late Cretaceous–Early Paleocene palaeobathymetric trends in the southwestern Barents Sea—Palaeoenvironmental implications of benthic foraminiferal assemblage analysis: Palaeogeography, Palaeoclimatology, Palaeoecology, v. 307, no. 1–4, p. 44–58, doi:10.1016/j.palaeo.2011.04.021.

Shephard, G. E., R. D. Müller, and M. Seton, 2013, The tectonic evolution of the Arctic since Pangea breakup: Integrating constraints from surface geology and geophysics with mantle structure: Earth-Science Reviews, v. 124, p. 148–183, doi:10.1016/j.earscirev.2013.05.012.

Sherwood, K. W., P. P. Johnson, J. D. Craig, S. A. Zerwick, R. T. Lothamer, D. K. Thurston, and S. B. Hurlbert, 2002, Structure and stratigraphy of the Hanna trough, US Chukchi shelf, Alaska, *in* E. L. Miller, A. Grantz, and S. Klemperer eds., Tectonic evolution of the Bering shelf–Chukchi Sea–Arctic margin and adjacent landmasses: Boulder, Colorado, Geological Society of America Special Paper 360, p. 39–66, doi:10.1130/0-8137-2360-4.39.

Smelror, M., and G. B. Larssen, 2016, Are there Upper Cretaceous sedimentary rocks preserved on Sørkapp Land, Svalbard?: Norsk Geologisk Tidsskrift, v. 96, doi:10.17850/njg96-2-05.

Smosna, R., K. R. Bruner, and A. Burns, 1999, Numerical analysis of sandstone composition, provenance, and paleogeography: Journal of Sedimentary Research, v. 69, no. 5, p. 1063–1070, doi:10.2110/jsr.69.1063.

Sokolov, S. D., G. Y. Bondarenko, O. L. Morozov, V. A. Shekhovtsov, S. P. Glotov, A. V. Ganelin, and I. R. Kravchenko-Berezhnoy, 2002, South Anyui suture, northeast Arctic Russia: Facts and problems, *in* E. L. Miller, A. Grantz, and S. L. Klemperer, eds., Tectonic evolution of the Bering shelf–Chukchi Sea–Arctic margin and adjacent landmasses: Boulder, Colorado, Geological Society of America Special Paper 360, p. 209–224, doi:10.1130/0-8137-2360-4.209.

Soloviev, A., A. Zaionchek, O. Suprunenko, H. Brekke, J. Faleide, D. Rozhkova, A. Khisamutdinova, N. Stolbov, and J. Hourigan, 2015, Evolution of the provenances of Triassic rocks in Franz Josef Land: U/Pb LA-ICP-MS dating of the detrital zircon from Well Severnaya: Lithology and Mineral Resources, v. 50, no. 2, p. 102–116, doi:10.1134/S0024490215020054.

Sømme, T. O., W. Helland-hansen, O. J. Martinsen, and J. B. Thurmond, 2009, Relationships between morphological and sedimentological parameters in source-to-sink systems: A basis for predicting semi-quantitative characteristics in subsurface systems: Basin Research, v. 21, no. 4, p. 361–387, doi:10.1111/j.1365-2117.2009.00397.x.

Steel, R. J., and D. Worsley, 1984, Svalbard's post-Caledonian strata—An atlas of sedimentational patterns and palaeogeographic evolution, *in* A. M. Spencer, ed., Petroleum geology of the north European margin: Dordrecht, the Netherlands, Springer, p. 109–135., doi:10.1007/978-94-009-5626-1_9.

Stephenson, R., A. Embry, S. Nakiboglu, and M. Hastaoglu, 1987, Rift-initiated Permian to Early Cretaceous subsidence of the Sverdrup basin, *in* C. Beaumont and A. J. Tankard, eds., Sedimentary basins and basin-forming mechanisms: Calgary, Alberta, Canada, Canadian Society of Petroleum Geologists Memoir 12, p. 213–231.

Stoupakova, A. V., E. Henriksen, Y. K. Burlin, G. B. Larsen, J. K. Milne, T. A. Kiryukhina, P. O. Golynchik, S. I. Bordunov, M. P. Ogarkova, and A. A. Suslova, 2011, The geological evolution and hydrocarbon potential of the Barents and Kara shelves, *in* A. M. Spencer, A. F. Embry, D. L. Gautier, A. V. Stoupakova, and K. Sørensen, eds., Arctic petroleum geology: Geological Society, London, Memoirs 2011, v. 35, p. 325–344, doi:10.1144/M35.21.

Syvitski, J. P. M., and J. D. Milliman, 2007, Geology, geography, and humans battle for dominance over the delivery of fluvial sediment to the coastal ocean: Journal of Geology, v. 115, no. 1, p. 1–19, doi:10.1086/509246.

Toro, J., E. L. Miller, A. V. Prokopiev, X. Zhang, and R. Veselovskiy, 2016, Mesozoic orogens of the Arctic from Novaya Zemlya to Alaska: Journal of the Geological Society, v. 173, no. 6, p. 989–1006, doi:10.1144/jgs2016-083.

Torsvik, T. H., and T. B. Andersen, 2002, The Taimyr fold belt, Arctic Siberia: Timing of prefold remagnetisation and regional tectonics: Tectonophysics, v. 352, no. 3–4, p. 335–348, doi:10.1016/S0040-1951(02)00274-3.

Torsvik, T. H., and L. R. M. Cocks, 2004, Earth geography from 400 to 250 Ma: A palaeomagnetic, faunal and facies review: Journal of the Geological Society, v. 161, no. 4, p. 555–572, doi:10.1144/0016-764903-098.

Tuchkova, M. I., S. D. Sokolov, A. K. Khudoley, V. E. Verzhbitsky, Y. Hayasaka, and A. V. Moiseev, 2011, Permian and Triassic deposits of Siberian and Chukotka passive margins: Sedimentation setting and provenances, *in* Proceedings of the International Conference on Arctic Margins VI: ICAM VI: Fairbanks, Alaska, May 31–June 2, 2011, p. 61–96.

Tuchkova, M. I., S. Sokolov, and I. R. Kravchenko-Berezhnoy, 2009, Provenance analysis and tectonic setting of the Triassic clastic deposits in western Chukotka, northeast Russia, *in* D. B. Stone, K. Fujita, P. W. Layer, E. L. Miller, A. V. Prokopiev, and J. Toro, eds., Geology, geophysics and tectonics of Northeastern Russia: A tribute to Leonid Parfenov: Stephan Mueller Special Publication Series 4, p. 177–200, doi:10.5194/smsps-4-177-2009.

Tugarova, M., T. Pchelina, N. Ustinov, and K. Viskunova, 2008, Lithological and geochemical characteristics of Triassic sediments from the central part of the South Barents depression (Arkticheskaya-1 well): Polar Research, v. 27, no. 3, p. 495–501, doi:10.1111/j.1751-8369.2008.00078.x.

Tullius, D. N., A. L. Leier, J. M. Galloway, A. F. Embry, and P. K. Pedersen, 2014, Sedimentology and stratigraphy of the Lower Cretaceous Isachsen Formation: Ellef Ringnes Island, Sverdrup Basin, Canadian Arctic archipelago: Marine and Petroleum Geology, v. 57, p. 135–151, doi: 10.1016/j.marpetgeo.2014.05.018.

Tye, R. S., J. P. Bhattacharya, J. A. Lorsong, S. T. Sindelar, D. G. Knock, D. D. Puls, and R. A. Levinson, 1999, Geology and stratigraphy of fluvio-deltaic deposits in the Ivishak Formation: Applications for development of Prudhoe Bay Field, Alaska: AAPG Bulletin, v. 83, no. 10, p. 1588–1623.

Verzhbitsky, V. E., and A. K. Khudoley, 2010, Western Laptev Sea region framework–Structural style and timing of deformation: 4th EAGE St. Petersburg International Conference and Exhibition on Geosciences—New Discoveries through Integration of Geosciences, St. Petersburg, Russia, April 5–10, 2010, doi:10.3997/2214-4609.20145418.

Verzhbitsky, V. E., S. D. Sokolov, E. M. Frantzen, A. Little, M. I. Tuchkova, and L. I. Lobkovsky, 2012, The South Chukchi sedimentary basin (Chukchi Sea, Russian Arctic): Age, structural pattern, and hydrocarbon potential, *in* D. Gao, ed., Tectonics and sedimentation: Implications for petroleum systems: AAPG Memoir 100, p. 267–290, doi:10.1306/13351557M1003534.

Vigran, J. O., G. Mangerud, A. Mørk, D. Worsley, and P. A. Hochuli, 2014, *in* Palynology and geology of the Triassic succession of Svalbard and the Barents Sea: Trondheim, Norway, Geological Survey of Norway Special Publication 14, 270 p.

Vyssotski, A. V., V. N. Vyssotski, and A. A. Nezhdanov, 2006, Evolution of the west Siberian Basin: Marine and Petroleum Geology, v. 23, no. 1, p. 93–126, doi:10.1016/j.marpetgeo.2005.03.002.

Whittaker, R. C., N. E. Hamann, and T. Pulvertaft, 1997, A new frontier province offshore northwest Greenland: Structure, basin development, and petroleum potential of the Melville Bay area: AAPG Bulletin, v. 81, no. 6, p. 978–998.

Zakharov, V., B. Shurygin, N. Kurushin, S. Meledina, and B. Nikitenko, 2002, A Mesozoic ocean in the Arctic: Paleontological evidence: Russian Geology and Geophysics, v. 43, p. 143–70.

Zhang, X., V. Pease, J. Skogseid, and C. Wohlgemuth-Ueberwasser, 2016, Reconstruction of tectonic events on the northern Eurasia margin of the Arctic, from U-Pb detrital zircon provenance investigations of late Paleozoic to Mesozoic sandstones in southern Taimyr Peninsula: GSA Bulletin, v. 128, p. 29–46, doi:10.1130/B31241.1.